

Deanship of Graduate Studies

Al-Quds University



**Effect of Electrolyte Concentration
On Colloidal Charge Reversal**

Reem Naim Afaneh

M.Sc Thesis

Jerusalem-Palestine

1433/2012

**Effect of Electrolyte Concentration
On Colloidal Charge Reversal**

Reem Naim Afaneh

Supervisor: Dr.Khawla Qamhieh

**This Thesis is Submitted in Partial fulfillment of
Requirement for the Degree of Master of Applied Industrial
Technology,
Al-Quds University**

1433/2012



Al-Quds University

Deanship of Graduate Studies

Applied and Industrial Technology Program

Thesis approval

Effect of Electrolyte Concentration

On Colloidal Charge Reversal

Prepared by: Reem Naim Afaneh

Registration No: 20724008.

Supervisor: Dr. Khawla Qamhieh

Master thesis submitted and accepted, date / /2012

The name and signature of examining committee member are as follows

- | | |
|--|----------------|
| 1- Head of Committee: Dr. Khawla Qamhieh | Signature..... |
| 2- Internal Examiner: Dr.Ibrahim Kayali | Signature..... |
| 3- External Examiner: Dr.Shukri Khalaf | Signature..... |

Jerusalem-Palestine

1433/2012

Dedication

I would like to dedicate this work to my mother, my father, my husband Younis Alzeer and my daughter Jana, my husband's mother, my husband's sister and my brothers and sisters in their encouragement and stimulation throughout the duration of my writing up.
..Thanks all...

Reem Afaneh

Declaration

I certify that this thesis submitted for the degree of Master is my own research, except where otherwise acknowledged, and that this thesis (or any part of the same) has not been submitted for higher degree to any other university or institution.

Signed:

Date:

Acknowledgment

Initially, I would especially like to thank my supervisor, Dr. Khawla Qamhieh who give me an opportunity to do this work in which I am really interested, and make this thesis possible. Thanks for her guidance, suggestions, and valuable help during the course of this work.

I owe thanks to a number of individuals in the department of Chemistry at the University of Jerusalem – Abu Deis both in general and with regard to my thesis.

I do not forget to thank my colleagues for their encouragement.

Very special thanks are also due to my mother Suhair Awwad and my father Naim Afaneh for all their guidance, support, and stimulation .

Great many thanks I would like to give to my devoted husband Younis. It has been his love and support (along with my children) that has provided me the incentive to complete my thesis. I sincerely cannot help expressing how I should credit this thesis to his support. I am extremely fortunate to have him in my life.

I am also very grateful to my husband's sisters Sanaa, Wafaa, And Remaa for their support, encouragement, stimulation and valuable help. They gave me confidence from the beginning and thus gave me the ability to continue studying and working hard. Thanks my love.

I am also greatly indebted to all my friends especially Mirfit Amleh who has helped and supported me in all possible ways as needed. Above all, I thank God for making all this possible.

Abstract:

The structure of the electric double layer (EDL) in contact with central charged sphere macroion surfaces is studied within the framework of the primitive model through Monte Carlo simulations. We studied the effects of salinity and valences on EDL structure. These effects were analyzed in terms of counterions accumulations profiles, charge densities, and electrostatic potentials.

As the valences rises the accumulated charge also increases, and also when the salt concentration increases the accumulated charge increases.

And as a result when the valences, sizes, and β values of counterions increased the absolute value of zeta potential was decreased to approach zero at large separation of charged surface, which affects the EDL structure and its thickness, which decreases as the valance increases.

At high salt concentration, the macroion becomes overcharged so that their apparent charge has been changed to the opposite sign of the original charge of the macroion, and the zeta potential calculated at shear plane ($r = 24 \text{ \AA}$) has also changed.

Table of Contents

Chapter one	
1. Introduction	2
1.1 Colloids	4
1.2 DLVO Theory	4
1.3 Electric double layers	6
1.4 Models of the electrical double-layer	7
1.4.1 Helmholtz model	7
1.4.2 Gouy- Chapman model	8
1.4.3 Stern-Graham model	8
1.5 Charge inversion	9
1.6 Computer simulations	10
1.7 Previous Studies	11
1.8 Statement of the problem	13
Chapter two	
2. Model and method	15
2.1 Model	15
2.2 Method and simulation	17
2.3 Metropolis algorithm	18
Chapter three	

3 Result and discussions	20
3.1 Systems without adding salt.	21
3.2 Effect of adding salt.	24
3.3 Critical surface charge density of the macroion	39
Chapter four	45
Conclusions	46
References	47

List of Tables

Table number	Table name	Page
Table 2.1	Name of the ensemble used in simulation.	18
Table 3.1	Values of the maximum accumulation of counterions g_{mi} in the vicinity of macroion for all charges distributions for counterion valence $Z_i= 1, 2, 3, 4$ and 5 .	22
Table 3.2	Values of Z_{acc} for the system with central charge distribution and at different counterion valences ($Z_i=1, 2, 3, 4, 5$) at $r=24 \text{ \AA}$	23
Table 3.3	Electrostatic potential with different counterion valences ($Z_i = 1, 2, 3, 4$ and 5)	25
Table 3.4	Accumulated charge for the system with different electrolyte at $\beta = 0.0, 0.75, 1.0, 2.5,$ and 6.25 .	34
Table 3.5	Electrostatic potential for the system with central charge distributions at counterion valence of $Z_i=1$ at different concentrations of salt.	37

List of Figures

Figure number	Figure name	Page
Figure 1.1	Distribution of positive and negative ions around the charged macroion in EDL.	3
Figure 1.2	DLVO-type interaction (continuous line) obtained as the sum of the electrostatic repulsion and van der Waals attraction.	5
Figure 1.3	The electrical double Layer structure near the surface of the positively charged particles	6
Figure 1.4	Schematic representation of the Helmholtz model of the electrical double-layer: (a) distribution of counterions in the vicinity of the charged surface; (b) variation of electrical potential with distance from the surface.	7
Figure 1.5	Schematic representation of the Gouy-Chapman model of the electrical double-layer: (a) distribution of counterions in the vicinity of the charged surface; (b) variation of electrical potential with distance from the surface.	8
Figure 1.6	Schematic representation of the Stern-Graham model of the electrical double-layer: (a) distribution of counterions in the vicinity of the charged surface; (b) variation of electrical potential with distance from the surface.	9
Figure 1.7	The connection between experiment ,theory ,and computer simulation	11
Figure 2.1	Schematic illustration of the macroion charge distributions: (a) a central charge with R_M denoting the macroion radius.	15
Figure 2.2	Metropolis algorithm is used to reject or accept a move.	18
Figure 3.1	Macroion-counterion radial distribution functions at counterion valences $Z_i = 1, 2, 3, 4$ and 5 .	21
Figure 3.2	Accumulated charge for the systems with different	23

	valence of counterion ($Z_i = 1, 2, 3, 4$ and 5).	
Figure 3.3	Electrostatic potential for the systems with different counterion valences ($Z_i = 1, 2, 3, 4$ and 5).	25
Figure 3.4	EDL potential as a function of counterion valence Z_i , (a) square points are Ψ_0 and (b) circle points are (zeta potential).	26
Figure 3.5	macroion- counterion rdfs at the indicated amount of simple a) 3:1 b) 4:1 c) 5:1 electrolyte expressed as the counterions to macroion charge ratio β at $Z_i = 1$ for the system with the central charge distribution.	28
Figure 3.6	macroion- coion rdfs at the indicated amount of simple a) 3:1 b) 4:1 c) 5:1 electrolyte expressed as the counterions to macroion charge ratio β at $Z_i = 1$ for the system with the central charge distribution.	30
Figure 3.7	macroion- anion rdfs at the indicated amount of simple a) 3:1 b) 4:1 c) 5:1 electrolyte expressed as the counterions to macroion charge ratio β at $Z_i = 1$ for the system with the central charge distribution.	31
Figure 3.8	Accumulated charge for the systems a) 3:1 b) 4:1 c) 5:1 electrolyte at different values of β . at $Z_i = 1$	33
Figure 3.9	Electrostatic potential for amount of simple a) 3-1 b) 4-1 c) 5-1 electrolyte at different values of β . at $Z_i = 1$.	36
Figure 3.10	Electrostatic potential for amount of simple 3:1, 4:1 and 5:1 electrolyte at $\beta = 2.5$.	36
Figure 3.11	Electrostatic surface potential for the system at different values of β (0, 0.75, 1, 2.5 and 6.25) at 3:1, 4:1 and 5:1 salt. At a) potential of the surface b) zeta potential equal.	38
Figure 3.12	zeta potential as a function of the colloidal surface charge density at different molar concentrations indicated in figures a - h, and Bjerrum length is 10.8 \AA .	43
Figure 3.13	scaled colloidal surface charge density as a function of the scaled concentration of 3:1, 4:1, and 5:1 electrolyte.	44

Abbreviations

c	Central (uniform) surface charge distribution.
DLVO theory	Derjaguin Landau-Verwey-Overbeek theory.
DNA	Deoxyribonucleic acid.
ϵ_0	The permittivity of vacuum = $8.854 * 10^{-12}$ c/v.m.
ϵ_r	The relative permittivity = 78.4 at room temperature 25°C
σ_M	Macroion surface charge density.
e	The elementary charge = $1.6 * 10^{-19}$ Coulomb.
EDL	Electric double layer .
MC	Monte Carlo .
NVE	Constant number of particles, volume and energy.
NVT	Constant number of particles, volume and temperature.
NPT	Constant number of particles, pressure and temperature.
PB	Poisson-Boltzmann .
rdfs	Radial distribution functions.
R_M	Macroion radius.
R_S	Radius of charged site.
R_i	Counterions radius.
R_{ca}	Cations radius.
R_a	Anions radius.
R_{sph}	Spherical cell radius.
ρ_i	Counterion number density.
ρ_M	Macroion number density.
Φ_M	Macroion volume fraction.
T	The temperature = 298 K in Kelvin.
U	Total potential.
U_{hs}	Hard-sphere repulsion.
U_{elec}	Coulomb interaction.

U_{ext}	External potential.
Z_M	Macroion charge.
Z_i	Counterions charge.
Z_{ca}	Cations charge.
Z_a	Anions charge.

Definitions

Colloids	Are defined as very small, finely divided solids (particles that do not dissolve) that remain dispersed in a liquid for a long time due to their small size and electrical charge.
Counterions	The small ions that have an opposite charge to the macroions.
Co-ions	The small ions that have a charge of the same sign of the macroions.
EDL	Is a structure that appears on the surface of an object when it is placed into liquid, this structure consists of two parallel layers of ions, one coincides to the object surface, and the other layer with counter charge sign in the fluid(diffuse layer).
Macroions	Stand for ions that are larger in radius and charge than other ions in the solution.
Monte Carlo simulations	It is stochastic technique (meaning it is based on the use of random numbers and probability statistics to investigate problems.
Primitive model	Model used to investigate intercolloidal structure of colloidal solutions. In this model, the charged colloids (referred to as macroions) and the small ions are both presented as hard spheres whereas the solvent is treated as a dielectric medium.
Charge Inversion	changing the net charge around the macroion surface due to the excess amount of counterions.
Zeta Potential	It is the potential differences between the dispersion medium and the stationary layer of fluid attached to the dispersed particle.

Chapter One

Chapter One

1. Introduction

Macroion is highly charged colloidal particle in water solution with multivalent

(Z valent) counterions (Z -ions). (Grosberg, 2002). They are important in biological systems, and charged membrane surfaces that are surrounded by charged molecules such as electrolyte ions and proteins. (Perutkova, 2010).

Electric double layer (EDL) structure is essential to predict the stabilization of colloidal dispersions and the properties of biological systems. It is available under appropriate physical and chemical conditions, charged interfaces display complex and counter-intuitive phenomena such as the charge inversion. (French, 2010). This phenomena have been extensively observed in different systems including DNAs, self assembled membranes and colloidal particles. (Gelbart, 2000 ; Angelini, 2003; Larsen , 1997; Tata, 2008) . A classical example in this case is the inversion of the electrostatic force between equally charged interfaces: charged surfaces which repel in presence of monovalent electrolyte develop strong electrostatic attractive forces in presence of multivalent counterions . (Moreira, 2001; Besteman, 2004). The case in which the counterions are multivalent is attracting a great experimental and theoretical interest due to their ability to induce complex and rich unique phenomena. (Lyklema, 2009).

Recent studies show that charge inversion has been reported to be largely independent of the chemical details of the system but it has been shown to strongly correlate with quantities such as the density of the charged interfacial groups and the valence of counterions. (Kjellander, 1992 ; Shklovskii , 2002 ; Levin, 2002 ; Jho, 2008).

The theoretical side the electrolyte solutions show that multivalent counterions develop strong correlations near surfaces with high charge density, which may be responsible for charge inversion.

EDL is consisted of an internal Stern layer, where some counter-ions are tightly bound to the charged interface, and an outer diffuse layer, where counter-ions exert thermal motions, that are shown in figure 1.1 The ion distributions in the diffuse layer are usually calculated using the Poisson-Boltzmann (PB) theory. (Gouy, 1910; Chapman 1913). Being of mean field nature, PB ignores the excluded-volume effects as well as electrostatic correlations of ions. It is popularly believed that PB failed in the presence of multivalent ions or highly charged interfaces. (Grosberg, 2002 ; Lau, 2002).

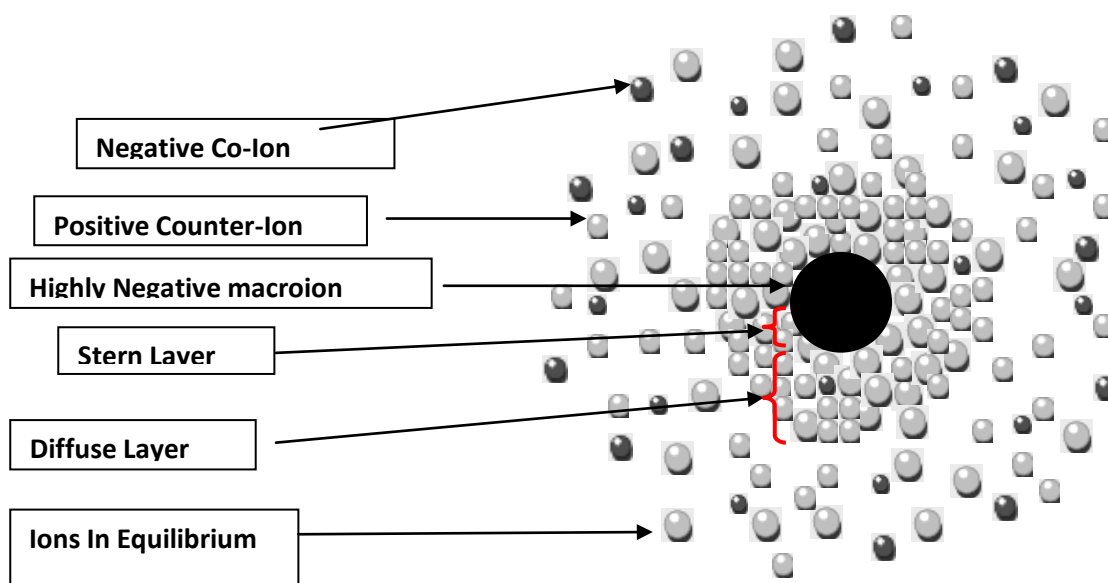


Figure (1.1): distribution of positive and negative ions around the charged macroion in EDL.

Poisson Boltzmann equation (Debye Huckel theory) says that the potential between two same charged macroions in the colloid mediated with their counterions always repulsive due to the ignoring ion-ion correlation. (Justice, 1975), (Chipman, 2003)

It is expected that the mean-field theory to be valid at separations comparable to the Debye length, when it is much larger than the Bjerrum length. At the same time the spatial correlation of fluctuations between the condensed charge and the surface charge on the same surface, which is over a distance comparable to or shorter than the Bjerrum length affects the local screening and charge inversion (J. G. Kirkwood, 1952). The simple case of a charged sphere immersed in a solvent with an electrolyte solution was tackled more than 60 years ago by Derjaguin, Landau, Verwey and Overbeek, (DLVO)(Verwey, 1948). They solved the Poisson-Boltzmann equation for the reduced electric potential. The DLVO theory predicts repulsion between an isolated pair of colloid particles at all separations, the attraction being due exclusively to nonelectrostatic London-van der Waals dispersion forces, which drive flocculation and coagulation processes whereas, the electrostatic repulsion imparts stability to the suspension.

Theoretically, the sources of like-charge attractions has been accounted by Sogami and Ise using a generalized Poisson-Boltzmann approach (Sogami, 1984). Later on some non-mean-field theory was developed (Gonzalez, 1998 ; Carbajal ,2002) following a self-consistent Ornstein-Zernike approach proposed by Zerah and Hansen.(Zerah,1968). The DLVO expression of the effective electrostatic energy, based on the Derjaguin approximation (Israelachvili, 1992), and works only for the situation that the screening

length is much smaller than the colloidal size. While this approximation fails in the salt-free case, they perform Monte Carlo simulations to re-verify this feature of attraction in the pure-energy part. (Chi-Lun, 2012).

Monte Carlo (MC) simulations are widely used hand in hand with different theoretical approaches describing point-like counter-ions (Hatlo and Lue 2009; Moreira and Netz 2002), and finite-sized counterions (Bhuiyan and Outhwaite 2009; Ibarra-Armenta et al. 2009; Tresset 2008) as well as the spatial distribution of charge within counter-ions and cations (Kim et al. 2008; May et al. 2008; Urbanija et al. 2008b).

1.1 Colloids

The term ‘colloid’ is derived from the Greek word ‘kolla’ for glue. It was originally used for gelatinous polymer colloids, which were identified by Thomas Graham in 1860 in experiments on osmosis and diffusion. Colloid science concerns systems in which one or more of the components has at least one dimension within the nanometre (10^{-9} m) to micrometre (10^{-6} m) range. If one of these states is finely dispersed in another then we have a ‘colloidal system’. These materials have special properties that are of great practical importance.

There are various examples of colloidal systems that include aerosols, emulsions, colloidal suspensions and association colloids. The simplest colloidal materials generally known as suspensions or dispersions, consist of two mixed phases. The continuous and dispersed phase it may be gas, liquid, or solid (or even plasma, the fourth phase of matter). Air, water, and plastics are common examples. The colloid particles make up the dispersed or suspended phase when uniformly distributed in the second, continuous phase. The dispersed matter may also be gas, liquid, or solid, and any combination in more complex suspensions. Colloidal dispersions are considered homogeneous mixtures even though they can be heterogeneous at or below the microscale.(Hunter, 2001) .

1.2 DLVO Theory

B. V. Derjaguin and L. D. Landau, E. J. W. Verwey and J. Th. G. Overbeek (DLVO) published their theory for describing the stability of lyophobic colloids in 1943 and 1948. (Lyklema,2005; Derjaguin,1941; Verwey, 1948). DLVO theory treats the interactions between lyophobic colloids in terms of two independent interactions: a repulsive electrostatic force, which arises due to charges on the particle surface, and an attractive van der Waals force due to the solid particle cores that shown in figure 1.2. The theory assumes a surface charge density σ_0 that is constant in regard to the electrolyte concentration and the counterion valency. (Evans,1999) The electrolyte affects the DLVO interaction only through the Debye length.

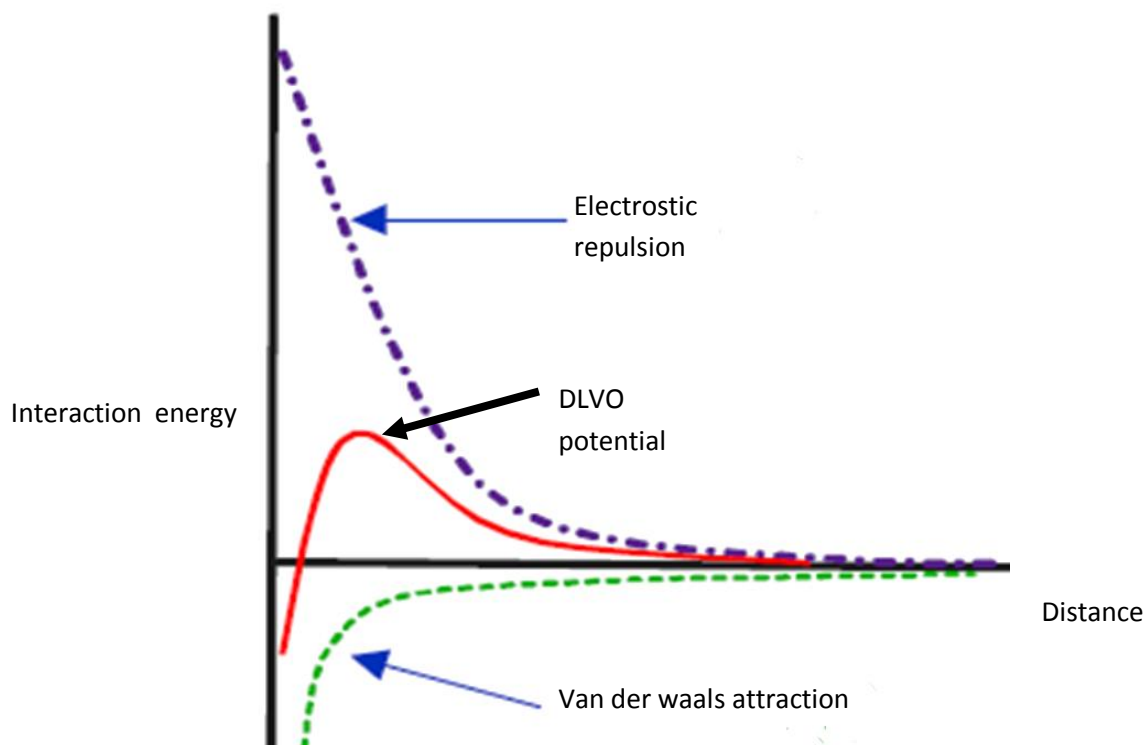


Figure (1.2): DLVO-type interaction (continuous line) obtained as the sum of the electrostatic repulsion and van der Waals attraction.

DVLO theory suggests that the stability of a particle in solution is dependent upon its total potential energy function V_T . This theory recognizes that V_T is the balance of several competing contributions:

$$V_T = V_A + V_R + V_S \quad \text{Eq(1.1)}$$

Where V_T the total potential energy, V_S : the potential energy due to the solvent.

V_R : the repulsive potential energy and V_A :the attractive potential energy.

$$U_a = -A / (12\pi D^2) \quad \dots\dots\dots \text{Eq(1.2)}$$

$$U_r = 2\pi\epsilon\xi^2 \exp (-kD). \quad \dots\dots\dots \text{Eq(1.3)}$$

Where A is Hamaker constant, D : particle of separation, π : solvent permeability,

K : function of the ionic composition, and ξ : zeta potential.

The Recent results of the molecular simulations have shown that, in the absence of van der Waals interactions, two isolated like-charged plates,(Guldbrand,1984) cylinders,(Gronbech, 1997) or spheres(Wu,1998) can be attractive at small separations in an electrolyte solution containing multivalent counterions. DLVO theory fails to account for such attraction because it neglects the charge density fluctuations in the electrostatic double layers.

1.3 Electric double layers

The electrical double layer is the cloud of ions with high local concentrations of counterions and low local concentrations of coions surrounding a charged surface. The thickness of the EDL is typically on the order of a few nanometers.

It is the structure formed by electrolyte ions around a charged surface, usually that of a colloid or electrode. An understanding of the EDL properties is a crucial matter for science and technology because of the large variety of related applications, that range from colloidal stability, electrokinetics and the description of biological systems to daily

manufactured products as inks, paint emulsions, foods or medicaments.(Fenell , 1994; Hiemenz, 1997).It is accepted (by chemists) Gouy-Chapman-Stern theory,

(Lyklema,1995);(Conway,1997).In the electrical double layer, oppositely charged particles attract each other and tend to collect at the surface of each substance but remain separated from one another by the finite size of each particle or by neutral molecules that surround the charged particles. The electrostatic attraction between the two opposite and separated charges causes an electrical field to be established across the interface.

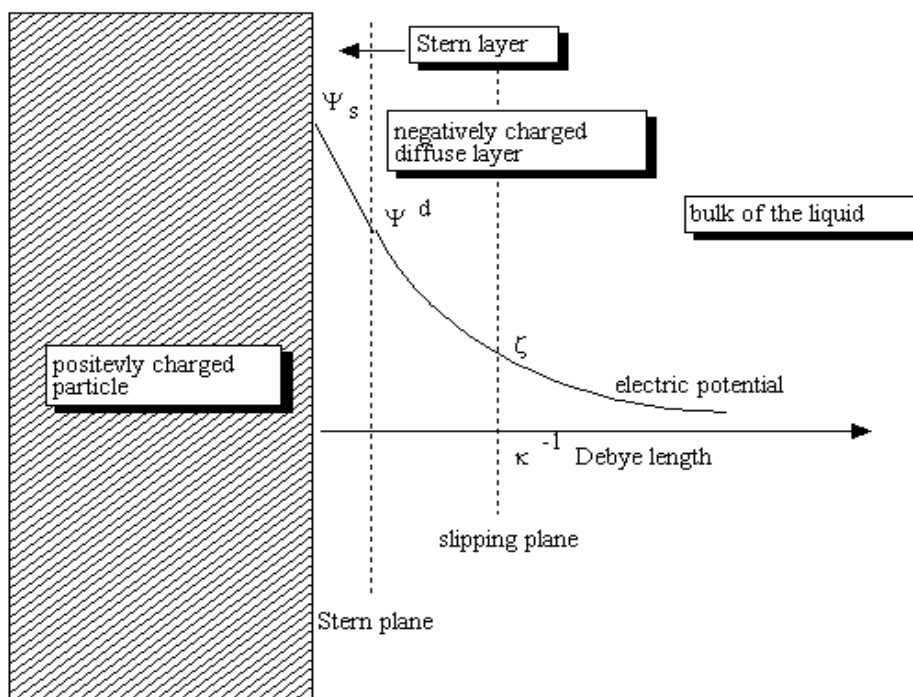


Figure 1.3 :the electrical double Layer structure near the surface of the positively charged particles

Some of the counterions might specifically adsorb near the surface and build an inner sub-layer, or so-called Stern layer in figure 1.3. The outer part of the screening layer is usually called the layer. The diffuse layer, move under the influence of thermal motion. There is a conventionally introduced slipping plane that separates mobile fluid from fluid that remains attached to the surface. Electric potential at the slipping plane is called electric potential or zeta potential. It is also denoted as ζ -potential. It is an abbreviation for electrokinetic potential in

colloidal systems. In the colloidal chemistry literature which is usually denoted using the Greek letter zeta, hence ζ -potential. This potential is difference between the dispersion medium and the stationary layer of fluid attached to the particle. A value of 24 mV (positive or negative) can be taken as the arbitrary value that separates low-charged surfaces from highly-charged surfaces in the colloid.^(Goodwin, 2004)

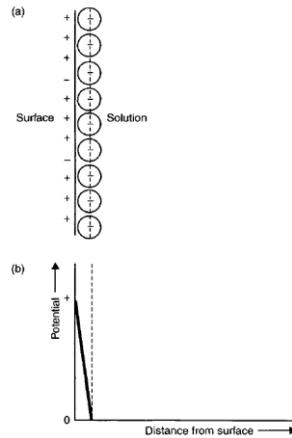
The term zeta potential(Hunter,1981) is intimately related to the Smoluchowski theories for electrophoresis. Since its defined so, zeta potential can not be directly measured, but can only be inferred indirectly from electrokinetic data, through the application of Smoluchowski theories.(Zecheng Gan, 2012).

1.4 Models of the electrical double-layer

1.4.1 Helmholtz model

In 1879, von Helmholtz proposed that all of the counterions are lined up parallel to the charged surface at a distance of about one molecular diameter (Figure 1.4).

The electrical potential decreases rapidly to zero within a very short distance from the charged surface in this model. Such a model treated the electrical double layer as a parallel-plate condenser, and the calculations of potential decay were based on simple capacitor equations. However, thermal motion leads to the ions being diffused in the vicinity of the surface, and this was not taken into account in the Helmholtz model.



Figure(1.4): Schematic representation of the Helmholtz model of the electrical double-layer: (a) distribution of counterions in the vicinity of the charged surface; (b) variation of electrical potential with distance from the surface.

1.4.2 Gouy- Chapman model

This model was proposed by Gouy (1910 ,1917) and Chapman (1913), consists of a diffuse distribution of the counterions, with the concentration of such ions falling off rapidly with distance near to the surface, due to the screening effect, then falling off gradually (Figure 1.5). Such a model is accurate for planar charged surfaces with low surface charge densities, and distances far away from the surface, but is inaccurate for surfaces with high surface charge densities, especially at small distances from the charged ones, since it treats the ions as point charges and neglects their ionic diameter.

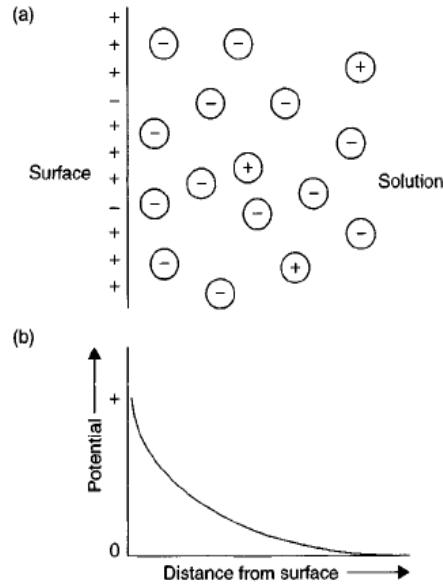
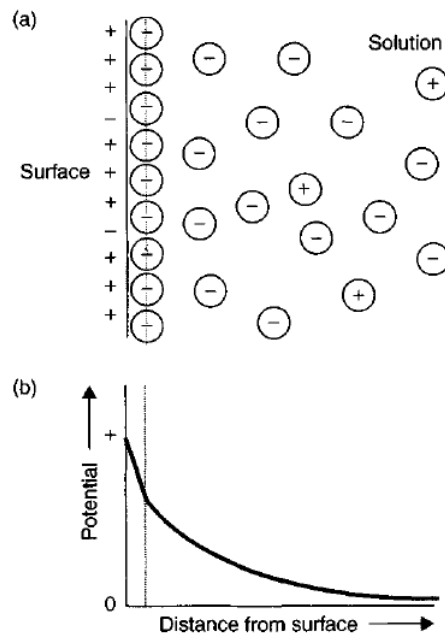


Figure (1.5): Schematic representation of the Gouy-Chapman model of the electrical double-layer: (a) distribution of counterions in the vicinity of the charged surface; (b) variation of electrical potential with distance from the surface.

1.4.3 Stern-Graham model

This model is shown in Figure(1.6), divides the stern doublelayer into two parts, i.e. (i) a fixed layer of strongly adsorbed counterions, adsorbed at specific sites on the surface, and (ii) a diffuse layer of ions similar to that of the Gouy-Chapman model. The fixed layer of ions is known as the Stern layer, and the potential decays rapidly and linearly in this layer. The potential decay is much more gradual in the diffuse layer. In the case of specifically adsorbing ions (multivalent ions, surfactants, etc.) the sign of the Stern potential may be reversed.



Figure(1.6): Schematic representation of the Stern-Graham model of the electrical double-layer: (a) distribution of counterions in the vicinity of the charged surface; (b) variation of electrical potential with distance from the surface.

1.5 Charge inversion (Overcharge)

Charge inversion is a phenomenon in which a charged particle (a macroion) strongly binds so many counterions in a water solution that its net charge changes sign.

At high concentrations of both di- and trivalent counterions accumulation of these ions occurs at the very proximity of the particle surface leading to charge reversal. The salt concentration at which charge reversal occurs is found to be always above the critical coagulation concentration.

Charge reversal (CR) or charge inversion (CI) have motivated a large number of studies in the past (Levin,2002; Gelbart,2000; Attard,1995; Deserno,2001; Tanaka,2001; Terao,2001; Terao,2002; Jimenez,2004; Messina,2000; Messina,2001; Messina, 2002; Nguyen,2000). These effects have been observed in the formation of self assembled polyelectrolyte layers on a charged substrate (.Decher,1997), self-assembled DNA-lipid

membrane complexes (adler,1997) and anomalous macroions adsorption on Lagmuir films (Cuvillier, 1998).

In general the electric mobility, is a complicated non-linear function of the electrokinetic ζ potential (Russel,1989; Joly, 2004). For small ζ and large ionic strengths, however, the relationship between the two is linear and is given by the Smoluchowski equation (Russel,1989; Hunter, 1981). A change in the sign of the ζ potential will, therefore, lead to the reversal of the electrophoretic mobility, conducted which will also associate with the overcharging (or the charge reversal) of the colloidal particles. (Qamhie and Lobaskin 2003), a computer simulation study of charge inversion in an asymmetric electrolyte treated by multivalent salt. They found that addition of multivalent salt caused macroion aggregation but when the inverted macroion charge becomes large enough the aggregation is redissolved, and enlarging the counterion valence increasing the effect of these phenomena.

(Holm et.al. (March)-2001) indicated that the charge inversion of EDLs with electrolyte mixtures can be described fairly well by using Integral Equations Theories and MC simulations ,they proved that the charge inversion depends on the ionic size chosen in the calculations.

For large salt concentrations, the reversal of the electrophoretic mobility will take place when the modulus of the colloidal surface charge density is larger than the critical value σ_c , which depends on the Bjerrum length, ionic radius, and the concentration of electrolyte.(Diehl and Levin,2008).

1.6 Computer simulations:

During the last decades a third methodological category between theory and experiment has been established in science and technology, the methodology of mathematical modelling and computer simulations. It can provide answers

in cases where theory faces its limits as in non-linear dynamics and chaos research or where experiments cannot be performed because of technical difficulties or economic reasons. By their nature, simulations are closer to experiment than theory. Computer 'experiments' differ from real experiments mainly by the fact that the real world is replaced by a model scenario.

Today, simulations are increasingly used for predicting properties of large chemical systems such as large molecules (biopolymers), molecules in solution, fluids and solids. The simulation results can only agree with the output of real experiments, when the model scenarios are closely related to reality, at least with respect to the relevant features.

Simulation is the numerical solution of equations, which mimic the behaviour of the system. Scientists interfere with the virtual reality of model objects *via* fast computer graphics visualisation and interactive manipulation of the scenario. Visualisation helps to gain qualitative insights and modify the model scenarios while interactive manipulation allows for directly controlling the model scenario: parameters can be changed.

Simulations in physical chemistry are made on different length and time scales, from atomistic to mesoscale, from femtoseconds to microseconds. Bridging different scales is one of the challenges in computer simulation today. Atomistic models describe the interactions between the models by quantum chemical approaches or by potentials derived from experimental findings.

Computer simulation makes use of these interactions by two basic technologies, Monte Carlo (MC) methods and molecular dynamics (MD) simulations.(Jürgen, 2001)

It explains the interactions between atoms, and the macroscopic properties of the system that show how the liquids behave. It has a valuable role to play in providing essentially exact results for problems in statistical mechanics which may be intractable to solve by model method .It is a test of theories that compared with real experiments result, this is clear in figure 1.7.(Schneider, 2003)

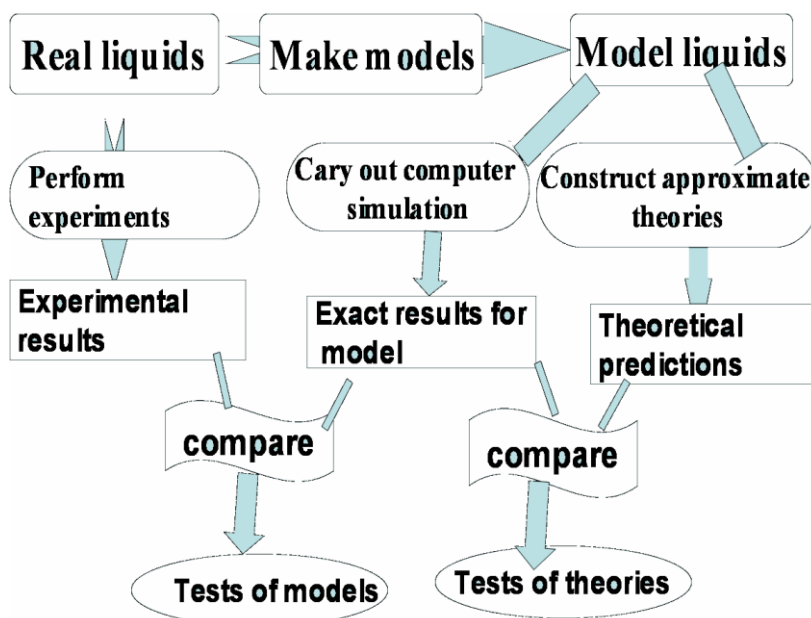


Figure 1.7 : The connection between experiment ,theory ,and computer simulation (Allen and Tildeslev 2001)

1.7 Previous Studies.

Many authors have revisited certain aspects of EDLs in the presence of different kinds of electrolytes. For instance, Boda et al. have analyzed the effect of the ion

size,(Messina,2005; Boda,2002) the effects of asymmetries ion diameters and charges.

(Henderson, 2004 , Henderson 2005) The consequences of an inhomogeneous dielectric coefficient discreteness of the solvent.

Other authors have studied the discreteness of the surface charge,(Ravindran,2004; Messina,2001; Messina,2002)whereas the role of excluded volume correlations has also been elucidated with the help of simulations in an advisable manner by Messina and co-workers.(Gonza ´lez-Tovar,2002).

The entropy of the solution decreases by enlarging the ion size, which enhances the interparticle correlations. Suspensions with trivalent (and even more highly charged) counterions have also been studied.(Quesada-Pe ´rez,2004; Tanaka M,2002; Mukherjee,2004).

Deserno et al. have studied a model of a rodlike polyelectrolyte molecule immersed into monovalent or divalent electrolyte by comparing results obtained from integral equation theories with those from molecular dynamics (MD)simulations. (Deserno,2001).

Mukherjee and co-workers have investigated the effect of mixed valence (mono- and divalent) counterions on the overcharging of a DNA-like spherocylindrical macroion.

(Mukherjee,2004).

Diehl and Levin have recently proposed a new dynamical definition of the effective colloidal charge for aqueous colloidal suspensions containing monovalent and multivalent counterions, which is particularly applicable to MC and MD simulations, (Diehl, A.; Levin,2004) whereas Qamhieh studied the mechanism of colloidal destabilization in the presence of highly asymmetric electrolytes.(Qamhieh,2003) Concerning charge inversion in model colloids, Martı ´n-Molina et al. examined experimentally the effect of the monovalent salts (in electrolyte mixtures) on the mobility reversal observed in suspensions of model polystyrene particles.(Martı ´n-Molina,2003)Some of their results were justified

by an integral equation theory including ion size correlations. Nevertheless, some matters, such as the failure of integral equation theories, remain unresolved.

A. Martín-Molina and C. Rodríguez-Beas study the effect of surface charge on colloidal charge reversal; they measured the electrophoretic mobility of latex particles (macroions) in the presence of a multivalent electrolyte. They have focused on the electrolyte concentration range at which a reversal in the electrophoretic mobility is expected to happen. (Martín-Molina,2009).

Madurga *et al.* (Madurga, 2007) compared different discretization models with the case of uniform surface charge distribution by charge density profiles, and reported interesting results in single electrolyte solution. Moreover, small ion distribution around one discretely charged surface immersed in electrolyte mixtures has also been examined by Taboada-Serrano *et al.* (Taboada-Serrano,2005) They showed that the exact distribution of the ions in the double layer region is determined by the balance of excluded volume and electrostatic interactions between ionic species of different sizes and valences.

In addition, Ravindran and Wu (Ravindran,2004) performed Monte Carlo simulations to investigate charge inversion of nanoparticles in single-salt solution. Their results were found to be qualitatively similar to those corresponding to a surface smeared charged model.

Most recently, Faraudo and Travasset (Faraudo,2007) explored many origins of charge inversion in electrolyte solutions by means of effects of discrete interfacial charges. Apart from the discretely charged head groups mentioned above, the biological interfaces between aqueous and hydrocarbon phases are characterized by a relatively large difference in their respective dielectric properties. Many studies have showed the effect of dielectric inhomogeneities on the behavior of macroions and their associated counterion distribution. (Bratko,1986;Lee,2009; Linse,2002; Wernersson,2007; Attard, 1988; Jho,2007; Netz , 1999; J. Reščič ,2008; Kanduč, 2007; Jho,2008; Henderson,2005)

Netz and co-workers (Netz, 2002; Fleck, 2007) highlighted that the effect of dielectric discontinuities on counterion collapse depends on how one deals with the surface charges. Using simple scaling arguments, Taheri-Araghi and Ha (Taheri-Araghi, 2005) found that the effect of image charges is intertwined with surface charge distributions.

These authors also suggested that the onset concentration for charge inversion is highly sensitive to the dielectric properties of the substrate, indicating that the in-plane correlations are more important in the presence of dielectric discontinuities.

Nguyen *et al.* (Nguyen ,2000)addressed that, on the basis of the strong correlated liquid (SCL) theory, the strength of charge inversion is markedly diminished once the charged surface is polarized.

Quite recently, Lopez-Garcia et al. (Lopez-Garcia,2010)have extended their previous model to allow for a different distance of closest approach to the particle surface for each ionic species. The most important fact is that it predicts charge reversal under appropriate circumstances by only considering such ionic excluded volume effects.

1.8 Statement of the problem

The aim of this study is to find out the effect of electrolyte concentration on electric double layers, which in turns will affect some properties of solutions containing macroions and their counterions. Also we want to determine the surface charge density of the macroion at ζ potential equal zero and to study the effect of salt concentration and counterion valences.

The thesis is organized as follows, chapter one contains the introduction. Chapter two describes the method and model settings for the simulations. Chapter three gives a detailed account of the results and discussion. And the conclusions are given in the final chapter.

Chapter Two

Model and Method

2. MODEL AND METHOD

2.1 Model

Monte Carlo simulation performed based on a primitive model of electrolyte solutions used in the framework of Mc-Millan–Mayer theory, i.e., the solvent is treated as a dielectric medium solely characterized by its relative permittivity ϵ_r equal to that of bulk water at T 298K. Whereas the colloids (later referred to as macroions), the counterions, cations and anions are represented by charged hard spheres.

Take solutions consisting of charged spherical macroions and counterions in a spherical cell with radius 100\AA containing one macroion at the center of the cell and relevant amount of counterions

$$N_I = |Z_M/Z_I| \times N_M \dots\dots\dots \text{Eq(2.1)}$$

Where N_I is the number of counterions, Z_M the charge of the macroion, Z_I is charge of the counterion and N_M : number of the macroion.

Throughout, macroions are represented as hard spheres with radius $R_M=20\text{\AA}$ and a total charge $Z_M=-60$, charged sites with radius R_S and charge $Z_S=-1$. The counterions are represented by charged hard spheres with radius $R_I=2\text{\AA}$ and charge $Z_I= +1, +2,+3,+4,+5$

At the same time, there is a macroion available which charges distribution such as continuous surface charge (the uniform macroion charge distribution) called central charge distribution; all N_S charges are localized at the center of the macroion.

I could find homogeneous surface charge density according to

$$\sigma_M = eZ_M/4\pi R_M^2 \text{ at } r=R_M \text{ see figure 2.1}$$

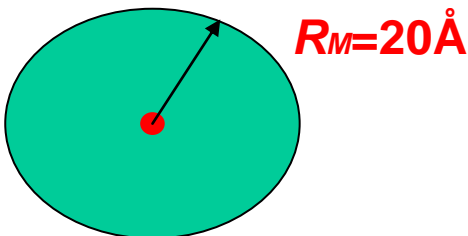


Figure 2.1: Schematic illustration of the macroion charge distributions a central charge with R_M denoting the macroion radius.

The total potential energy of the system U is

$$U = U_{hs} + U_{elec} + U_{ext} \dots\dots\dots \text{Eq(2.2)}$$

The hard sphere repulsion U_{hs} is given by

$$U_{hs} = \sum U_{ij}^{hs} (r_{ij}). \dots\dots\dots \text{Eq(2.3)}$$

$$U_{ij}^{hs} (r_{ij}) = \begin{cases} \infty, & r_{ij} < R_I + R_j. \dots\dots\dots \\ 0, & r_{ij} \geq R_I + R_j. \end{cases} \text{Eq(2.4)}$$

With R_I denoting the radius of particle I (a macroion, a macroion site, or a counterion, coion and anion) and r_{ij} the distance between the centers of particles I and j.

$$U^{elec} = \sum U_{ij}^{elec} (r_{ij}). \dots\dots\dots \text{Eq(2.5)}$$

$$U_{ij}^{elec} (r_{ij}) = Z_1 Z_2 e^2 / 4\pi\epsilon_0\epsilon_r r_{ij}. \dots\dots\dots \text{Eq(2.6)}$$

Where Z_I is the charge of particle I (a macroion site or a counterion, coion and anion), e the elementary charge, ϵ_0 the permittivity of vacuum, and ϵ_r the relative permittivity of water.

$$U_{ext} = \sum U^{ext} (r_I). \dots\dots\dots \text{Eq(2.7)}$$

With

$$U^{ext} (r_i) = \begin{cases} 0, & r_i \leq R_{sph} \quad \text{for a spherical cell.} \dots\dots\dots \\ \infty, & r_i > R_{sph} \end{cases} \text{Eq(2.8)}$$

$$U^{ext} (r_i) = 0, \dots\dots\dots \text{Eq(2.9)}$$

The mean electrostatic potential at distance r from the colloidal particle is then calculated as

$$\Psi_{EDL} = \int_R^{\infty} \frac{e}{4\pi\epsilon_0 \epsilon_r} \frac{Z_{acc}}{r'^2} d r' \quad \text{Eq(2.10)}$$

$P(r)$ is the integrated charge (in units of q) within a distance r from the center of the colloidal particle.

$$Z_{acc} = -Z + \int_R^r \sum Z_i \rho_i(r') 4\pi r'^2 dr' \quad \text{Eq (2.11)}$$

$P(r)$ is the integrated charge (in units of q) within a distance r from the center of the colloidal particle, i refers to the type of the microion.

Throughout, the system is considered at the macroion number density $M=2.510*10^{-7} \text{ \AA}^{-3}$, corresponding to a macroion volume fraction $M=0.0084$. The temperature $T=298 \text{ K}$ and the relative permittivity $=78.5$ were used. At these conditions, the Bjerrum length, denoting the distance between two unit charges at which the Coulomb interaction is equal to the thermal energy, becomes 7.15 \AA .

2.2 Method and simulation

The method which has been used to study the effect of the charge distribution and counterions size on the properties of electric double layer is Monte Carlo (MC) simulation, in the canonical ensemble, at constant number of particles, volume, and temperature according to the standard Metropolis algorithm. The configurations were generated by first placing the macroion in the center of the spherical cell. The macroion charges were positioned according to the different charge distributions. Finally, the counterions were positioned randomly $2*10^6$ attempted MC moves per particles were made in the production runs. All the simulations were performed using the integrated Monte Carlo/molecular dynamics/ Brownian dynamics simulation package MOLSIM. (Linse 2004)

Monte Carlo simulation is named after the city in Monaco, where the primary attractions are casinos that have games of chance. Gambling games, like roulette, dice, and slot machines which exhibit random behavior.

The use of MC methods to model physical problems allows us to examine more complex systems than we otherwise can. Solving equations which describe the interactions between two atoms is fairly simple; solving the same equations for hundreds or thousands of atoms is impossible. With MC methods, a large system can be sampled in a number of random configurations, and that data can be used to describe the system as a whole.

Table 2.1: Name of the ensemble used in simulation.

constraints	Name of the ensemble	states
NVE	Micro-canonical	Constant number of particles ,volume and energy
NVT	Canonical	Constant number of particles ,volume and temperature
NPT	Isothermal-isobaric	Constant number of particles, pressure and temperature

2.3 Metropolis Algorithm

In 1953 Metropolis made the first paper on a technique that was central to the method now known as simulated annealing, this paper showed the first numerical simulations of a liquid. The algorithm for generating samples from the Boltzmann distribution, he is credited as part of the team that came up with the name Monte Carlo method in reference to a colleague's relative's love for the Casinos of Monte Carlo. Monte Carlo methods are a class of computational algorithms that rely on repeated random sampling to compute their results. In statistical mechanics applications prior to the introduction of the Metropolis algorithm, the method consisted of generating a large number of random configurations of the system, computing the properties of interest (such as energy or density) for each configuration, and then producing a weighted average where the weight of each configuration is its Boltzmann factor.

It is implemented using the following algorithm:

- 1- Chose the particles to move at random and move them by a (random) distance.
- 2- Calculate the energy difference $\Delta U_{trial} = U_{new} - U_{old}$ between the old and the new configuration.

If $\Delta U_{trial} \leq 0$ accept the new configuration, else if random number generating $0 \leq x \leq 1$

is smaller than $\exp(-\Delta U_{trial} / K_B T)$, accept the move, else reject the move and count the old configuration as the new configuration. After every step , data for averages is accumulated before a new trial move is attempted.

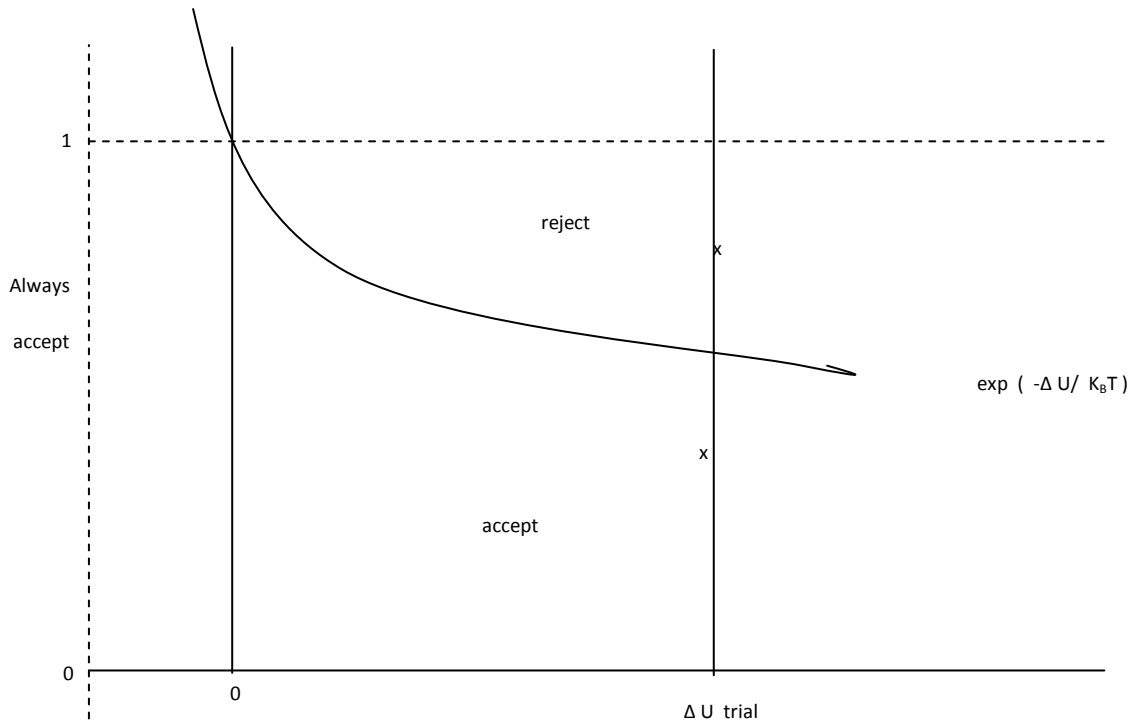


Figure 2.1: Metropolis algorithm is used to reject or accept a move.

$$\Delta U_{\text{trial}} = U_{\text{new}} - U_{\text{old}}$$

Chapter Three

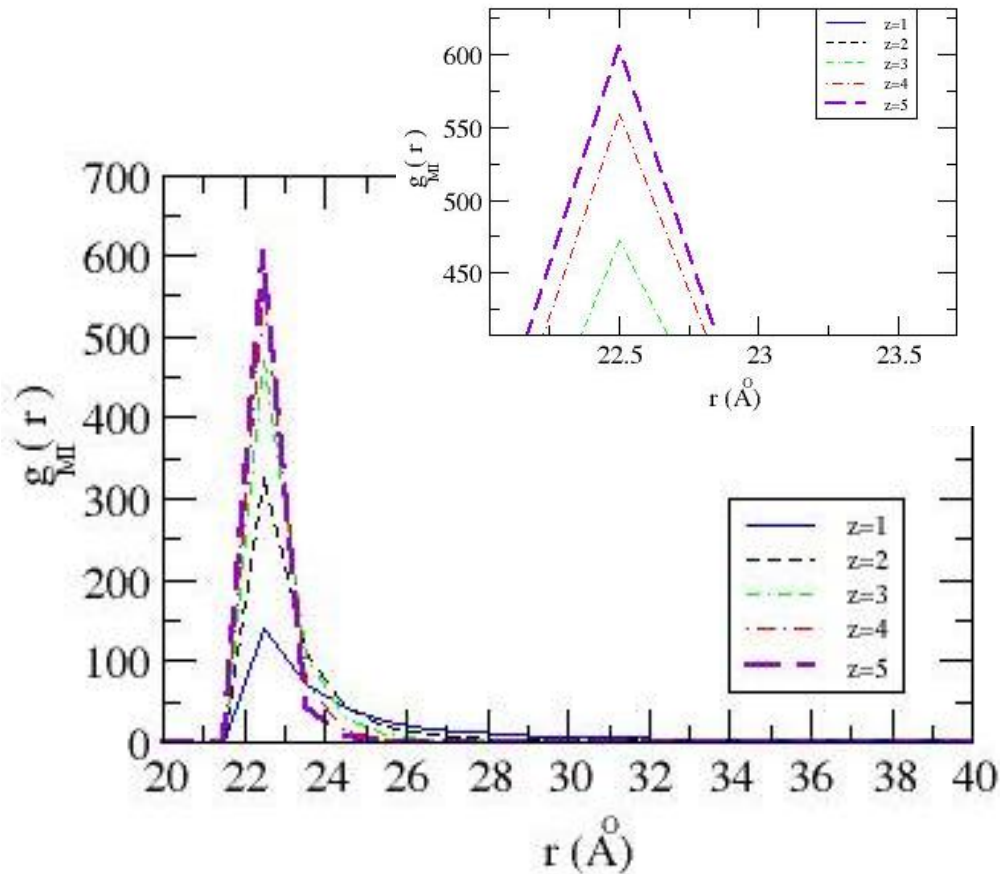
Results and Discussion

3 Results and discussion

3.1 Systems without adding salt

Macroion-counterions radial distribution functions (rdfs) for the central charge distributions with different counterion valences are shown in figure 3.1, rdfs obtained from a spherical cell that describe the distribution of counterions near a single macroion.

The rdf provides the relative density of small ions at distance r from the macroion. Its value being unity in the absence of any spatial correlation. From the figure, it is clear that when the counterion valence increased the accumulation of counterions around the macroion also increased at different counterion valences ($Z_i = 1,2,3,4,5$).



Figure(3.1): Macroion-counterion radial distribution functions at counterion valences

$Z_i = 1, 2, 3, 4$ and 5 .

Figure 3.1 shows that the electrostatic correlation between macroion and counterions which has the highest value at the valence that equal 5, then valence 4. Finally, the less electrostatic correlation are found in the monovalent counterions.

Table 3.1: Values of the maximum accumulation of counterions g_{mi} in the vicinity of macroion for macroion counterion radial distribution functions at counterion valence $Z_i= 1, 2, 3,4$ and 5 .

Valence (Z_i) of counterions	Maximum accumulation of counterions g_{mi}
1	143
2	325
3	473
4	559
5	604

In table 3.1 there is clear that the maximum value of accumulation is the highest in counterion valence $Z_i=5$.

The electrical double layer (EDL) is formed due to the accumulation of charge at the interface of a metal surface in contact with an electrolyte. The total charge in the EDL compensates the charge on the metal surface.

Accumulated charge (Z_{acc}) is the net charge of macroion, as well as counterions and coions bound to the macroion, it is calculated according to the equation below:

$$Z_{acc} = -Z + \int_R^r \sum Z_i \rho_i(r') 4\pi r'^2 dr' \quad \text{Eq(3.1)}$$

Z_i is the number of charge of any ion (counterion, coion, or cation), ρ_i the macroion number density, and r' is the distance between the center of macroion and counterion.

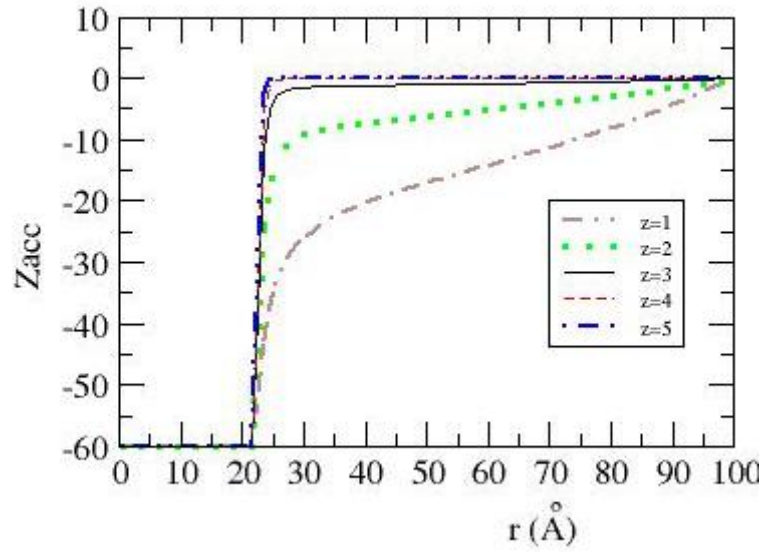


Figure 3.2: Accumulated charge for the systems with different valences of counterion ($Z_i = 1, 2, 3, 4$ and 5).

In figure 3.2, at $r = 24 \text{ \AA}$, the value in the case of $Z_i = 5$ is the highest than the others. As the counterions valences increase the accumulated charge increase.

Table 3.2: Values of Z_{acc} for the system with central charge distribution and at different counterion valences ($Z_i=1, 2,3,4,5$) at $r = 24 \text{ \AA}$.

Valence(Z_i)	Z_{acc} at $r=24 \text{ \AA}$
1	-40
2	-21
3	-8
4	-3
5	-2

Table 3.2 shows the value of accumulated charge at specific distance, the result shows that the value of accumulated charge increases when the counter ion valences increase.

By using accumulated charge we can calculate the EDL potential (Ψ_{EDL}) according to the following equation

$$\Psi_{EDL} = \int_R^{\infty} \frac{e}{4\pi\epsilon_0 \epsilon_r} \frac{Z_{acc}}{r'^2} d r' \quad \text{Eq(3.2)}$$

Where e is elementary charge, r' the distance between the center of macroion and counterion of particles, ϵ_0 : the permittivity of vacuum, and ϵ_r : the permittivity of water (78.4).

The development of a net charge at the particle of macroion surface affects the distribution of ions in the surrounding interfacial region, resulting in an increased concentration of counter ions (ions of opposite charge to that of the particle) close to the surface. Thus an electrical double layer exists around each particle.

The significance of zeta potential is that its value can be related to the stability of colloidal dispersions (e.g., a multivitamin syrup). The zeta potential indicates the degree of repulsion between adjacent, similarly charged particles (the vitamins) in a dispersion.

Zeta potential is electric potential in the interfacial double layer at the location of the slipping plane versus a point in the bulk fluid away from the interface. In other words, zeta potential is the potential difference between the dispersion medium and the stationary layer of fluid attached to the dispersed particle.

The total charge of the double layer is zero, but as the charges are spatially oriented and not randomly organized, they give rise to an electrical potential. The potential at any point on the double layer being defined (from the study of static electricity) as the work done in bringing unit charge from infinity to that point, in this study the point is at 60 \AA .

The variation of potential is very rapid. It changes sign near the colloidal surface and reaches maximum at $r = R_M + 2a$. Where r is the distance between the center of macroion and center of counterion, a is the radius of counterion, and R_M radius of macroion, this study has been taken by many authors such as. (Qamhieh, 2007), (Levin, 2008).

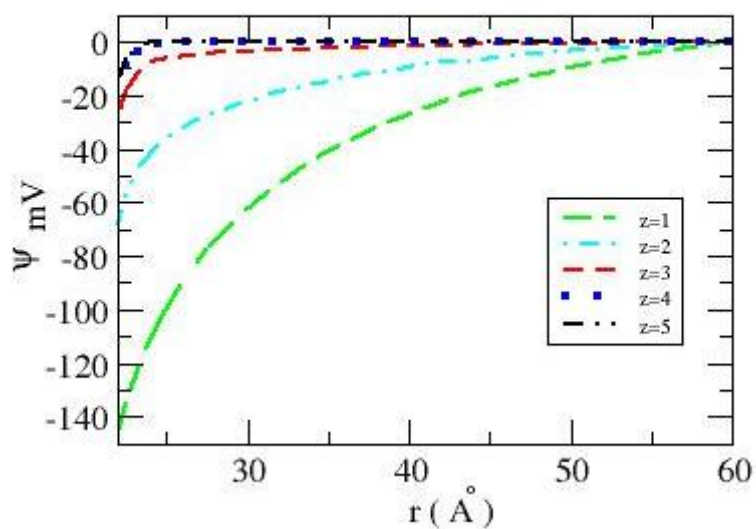


Figure 3.3: Electrostatic potential for the systems with different counterion valences ($Z_i = 1, 2, 3, 4$ and 5).

In figure 3.3, when the valences of ions increases the electrostatic potential increase, and also be a significant change in potential at $z = 1$, while a simple change at $z = 5$

Table 3.3: Electrostatic potential with different counterion valences ($Z_i = 1, 2, 3, 4$ and 5)

Valence(Z_i)	Ψ_0 (mV) at $r=22 \text{ \AA}$	Zeta potential (mV) at $r=24 \text{ \AA}$
1	-146	-112
2	-68	-42
3	-28	-8
4	-18	-1
5	-16	-0.39

From table 3.3 the values of surface electrostatic potential ψ_0 on the macroion surface increase as the $Z_i=5$, similar happened on potential of the diffuse part.

The potential at the surface of macroion (ψ_0) has been taken at (22 Å), while at (24 Å) for Zeta potential.

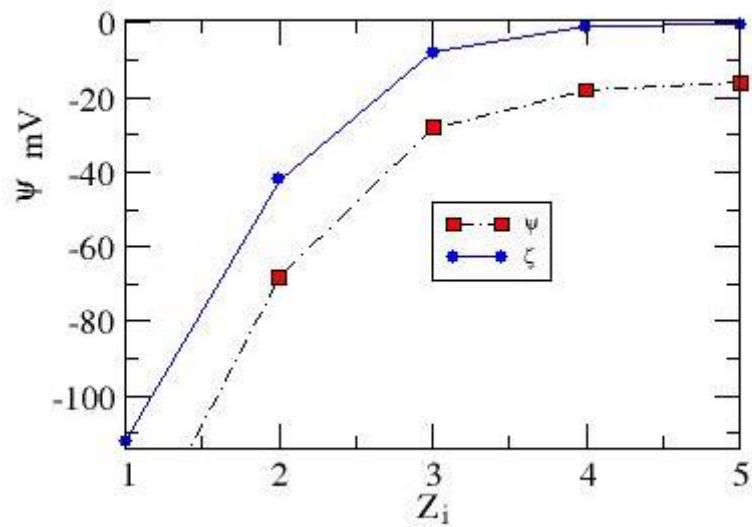


Figure 3.4: EDL potential as a function of counterion valence Z_i , (a) square points are Ψ_0 and (b) circle points are (zeta potential).

In figure 3.4 the electrostatic potential increases when Z_i increases at potential of surface and zeta potential, its value close to zero at high value of counterion valences.

When the values of counterions are small the change of potential is large then it become fixed at high value of concentration.

3.2 Effect of adding salt

The affect of adding salt on the properties in electrical double layer appears after adding (amount of simple as multivalent salt), where multivalent charge to the macroion charge ratio expressed by β value as in the equation below .

Where the value of β is calculated as

$$\beta = N_{ca} Z_{ca} / N_M Z_M \quad \text{Eq.(3.3)}$$

N_{ca} is the number of multivalent counterions (cation), Z_{ca} is the charge of multivalent counterion (cation), N_M is the number of macroion, and Z_M is charge of macroion.

When the salt has been added, it has been ionized to multivalent counterions and the coions(-1) affects the vicinity of monovalent counterions, impeding their entity, and causing inversion in the macroion net charge which counters the correlation between the macroion and counterions from attraction to repulsion, this phenomena is called charge inversion or (overcharge).

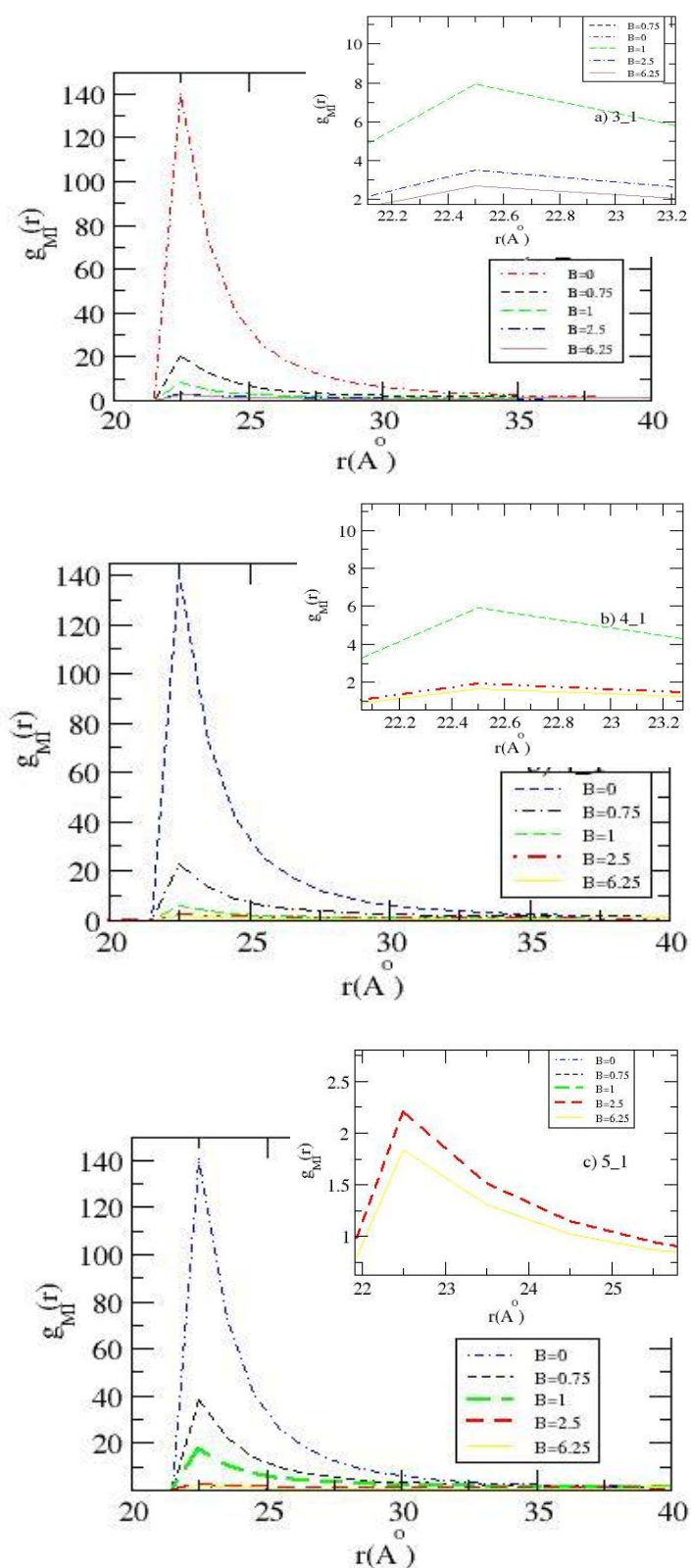
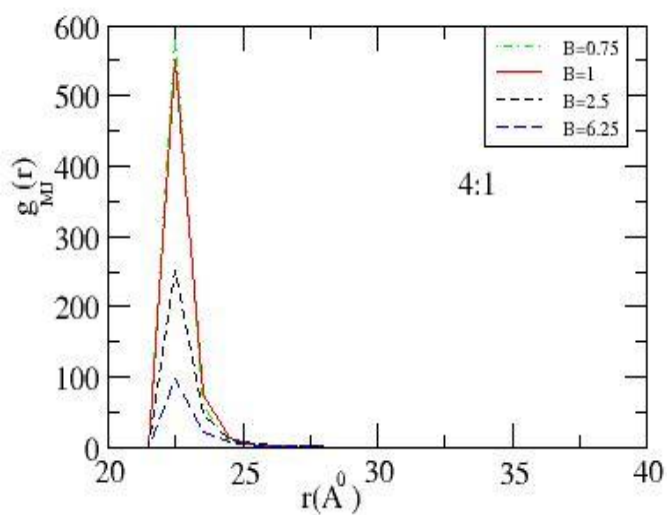
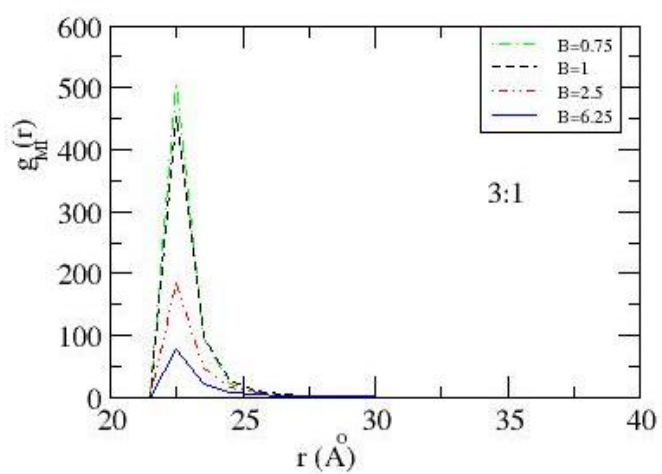


Figure 3.5: macroion- counterion rdfs at the indicated amount of simple a) 3:1 b) 4:1 c) 5:1 electrolyte expressed as the counterions to macroion charge ratio β at $Z_i = 1$ for the system with the central charge distribution.

Figure 3.5 shows the distribution of multivalent counterions (3:1,4:1,5:1) around the macroion, these results showed when the salt concentration increased the accumulation of multivalent counterions around the macroion is decreased.

Figure 3.6 shows the distribution of salt Cation near the macroion and it is clear that when the salt concentration increases the salt ion vicinity decreases.



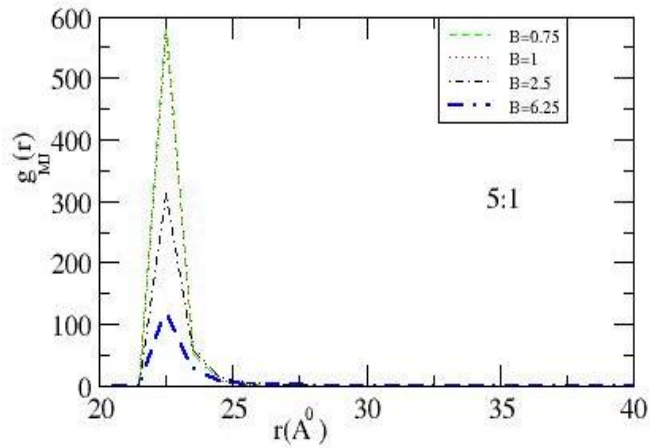
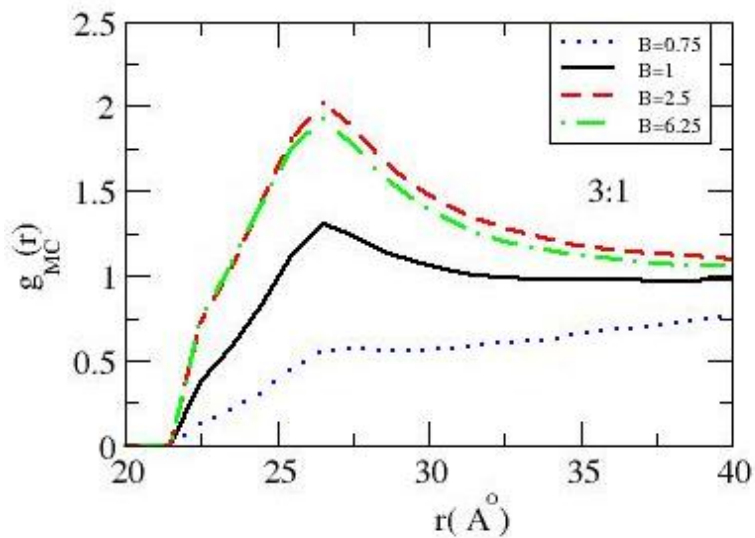


Figure 3.6: macroion- cation rdfs at the indicated amount of simple a) 3:1 b) 4:1 c) 5:1 electrolyte expressed as the counterions to macroion charge ratio β at $Z_i = 1$ for the system with the central charge distribution.

At low salt concentration the macroion-anion rdfs is reduced because of trivalent counterions adsorption on the stern layer as it has been shown in figure 3.7. At high salt concentration at $\beta = 2.5$ and $\beta = 6.25$ the macroion become overcharged and their apparent charge has the opposite sign so the ions correlation with macroion change, the coions expel the multivalent counterions and take their place.

a)



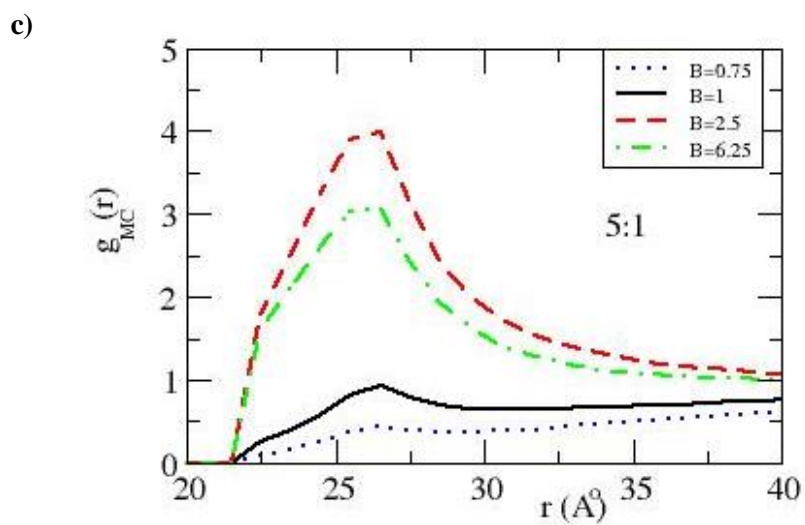
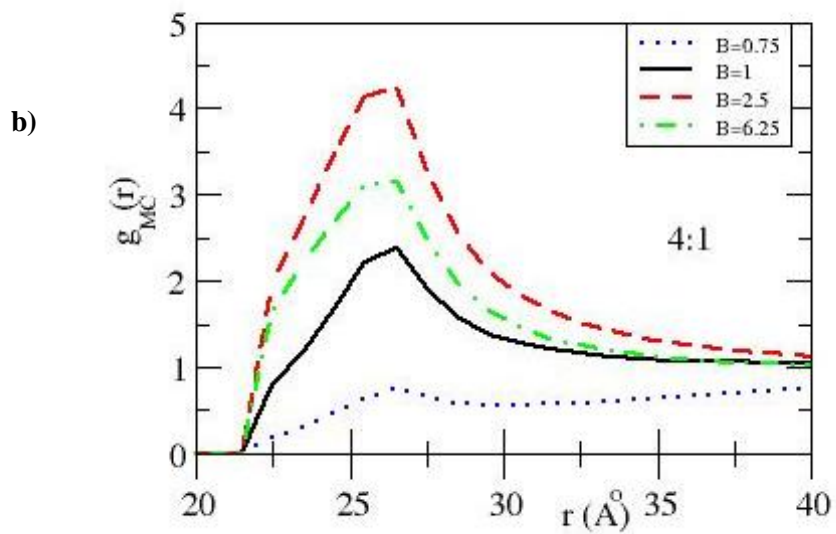
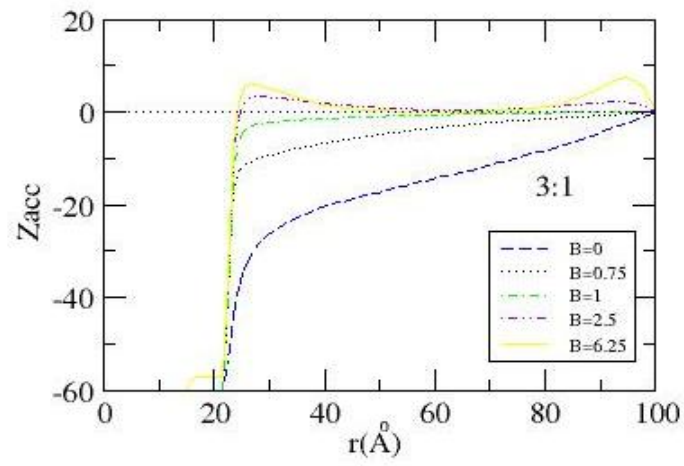
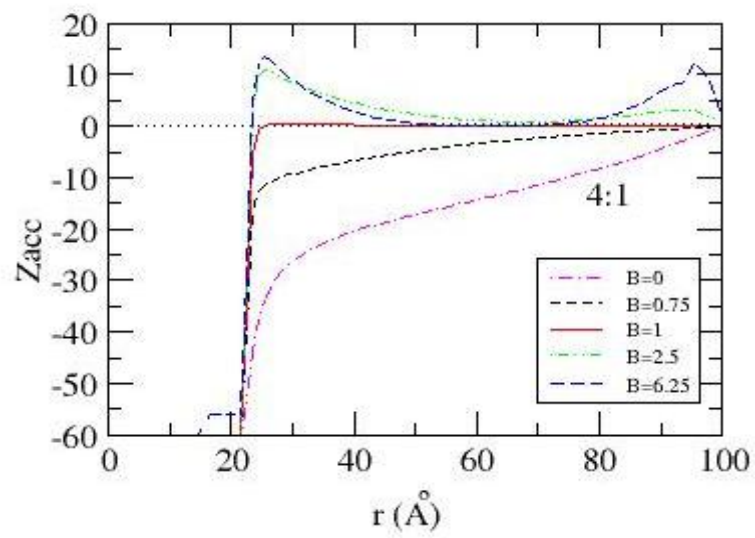


Figure 3.7: macroion- anion rdfs at the indicated amount of simple a) 3:1 b) 4:1 c) 5:1 electrolyte expressed as the counterions to macroion charge ratio β at $Z_i = 1$ for the system with the central charge distribution.

(a)



(b)



(c)

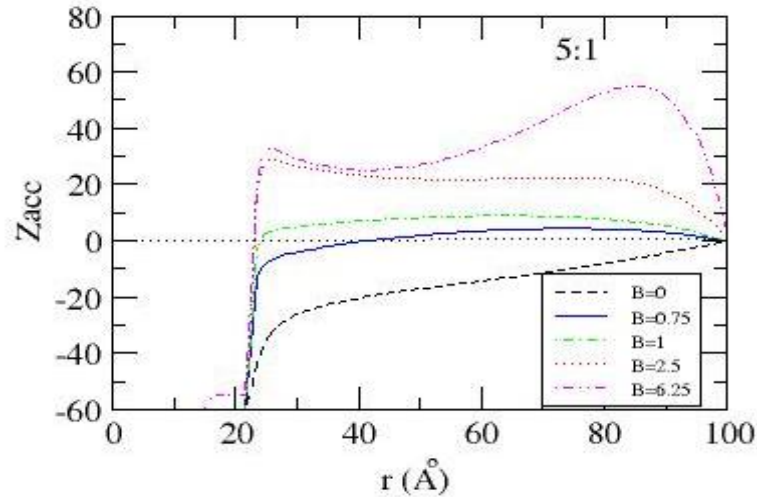


Figure 3.8: Accumulated charge for the systems a) 3:1 b) 4:1 c) 5:1 electrolyte at different values of β . at $Z_i = 1$

The effect of adding salt on the accumulated charge of the macroion is shown in figure 3.8.

When we add salt concentration 3:1 the charge inversion is occur few while at 5:1 it become high at different values of β (example at $\beta = 6.25$ the Z_{acc} in 3:1 is -3 while 4:1 is 8 and 5:1 is 25 at $r=24 \text{ \AA}$).

Table 3.4 shows how the excess amount of salt changes the sign of charged accumulated around the macroion surface, it has been taken at 24 \AA because the potential is calculated at shear plane when the Z accumulated equal Z effective.

These results show that when the salt concentration increases the accumulated charge increases.

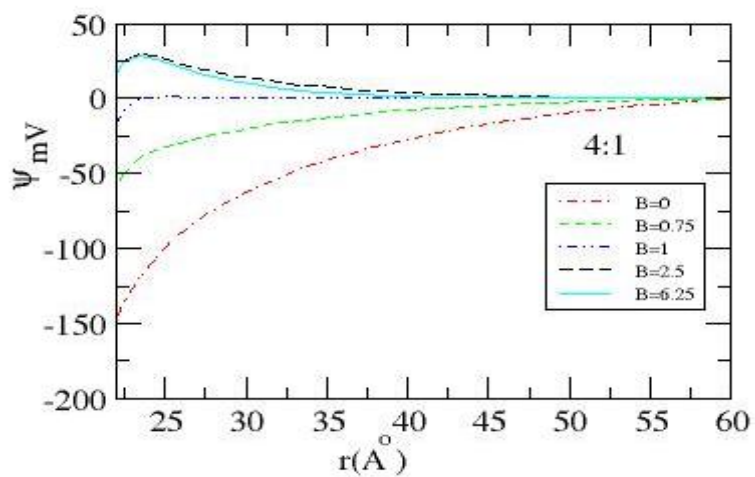
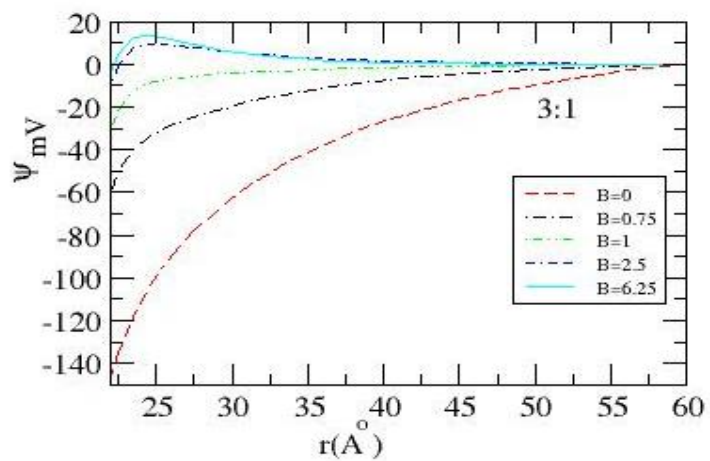
It was shown that the charge inversion was clear at 5:1 then in 4:1 and finally in 3:1.

At the same concentration of salt the charge inversion is observed in the highest valency 6.25 and there is no charge inversion in $\beta=0$

Table 3.4: Accumulated charge for the system with different electrolyte at $\beta = 0.0, 0.75, 1.0, 2.5$ and 6.25 .

Counterion valence	Electrolyte counterion	β value	Z_{acc} at $r=24 \text{ \AA}^0$
$Z_1 = 1$	3:1	0.0	-41
		0.75	-14
		1.0	-9
		2.5	-5
		6.25	-3
	4:1	0.0	-41
		0.75	-14
		1.0	-2
		2.5	7
		6.25	8
	5:1	0.0	-41
		0.75	-11
		1.0	1
		2.5	22
		6.25	25

The effect of adding salt on potential is shown in figure 3.9 at different values of β , it was cleared that when the concentration of salt is 5-1, the charge inversion occurs, and when the concentration of salt is 3-1 the inversion of charge does not happened at $r=24 \text{ \AA}$.



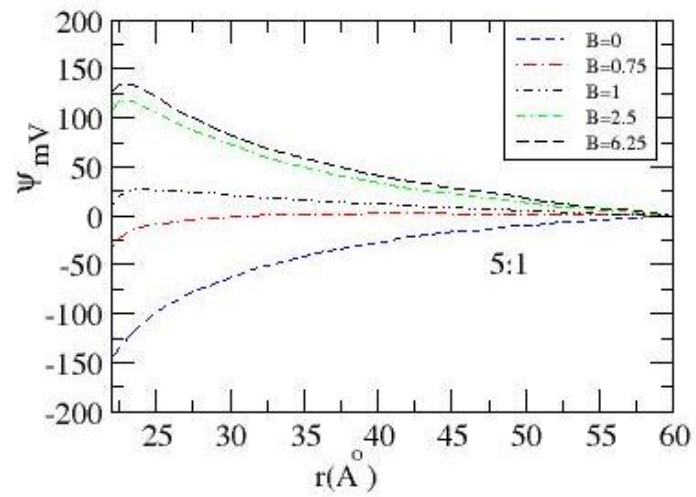


Figure 3.9: Electrostatic potential for amount of simple a) 3-1 b) 4-1 c) 5-1 electrolyte at different values of β . at $Z_i = 1$.

In figures 3.9, 3.10, it is noticed that the charge inversion was very clear in high salt concentration (5:1), and it is little lower in (3:1) at β equal 2.5.

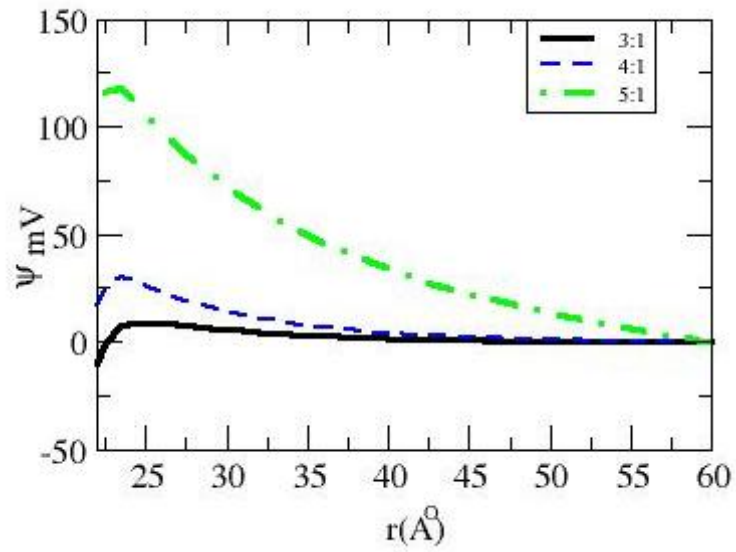


Figure 3.10: Electrostatic potential for amount of simple 3:1, 4:1 and 5:1 electrolyte at $\beta=2.5$.

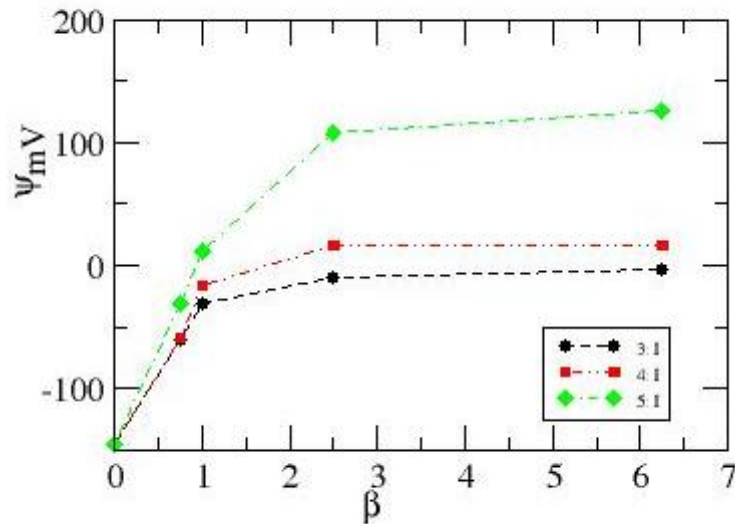
In figure 3.10 the value of electrostatic potential is 114 at 5:1 while in 4:1 is 29 and 3:1 is 8, so the charge inversion is clear in 5:1 then 4:1 and 3:1, then the lines are fixed at $r=60\text{\AA}$.

Table 3.5: Electrostatic potential for the system with central charge distributions at counterion valence of $Z_i=1$ at different concentrations of salt.

Counterion valence	Electrolyte counterion	β value	Ψ_0 Surface potential at 22 Å (mV)	zeta potential at 24 Å (mV)
$Z_i = 1$	3:1	0.0	-146	-112
		0.75	-60	-37
		1.0	-31	-10
		2.5	-10	+8
		6.25	-4	+12
	4:1	0.0	-146	-112
		0.75	-59	-37
		1.0	-16	0.5
		2.5	16	29
		6.25	16	28
	5:1	0.0	-146	-112
		0.75	-32	-11
		1.0	11	26
		2.5	108	114
		6.25	126	130

In table 3.5, there are different values for ψ_0 at $r = 22 \text{ \AA}$ and zeta potential at $r = 24 \text{ \AA}$ at different concentrations of β . The result shows that there is no charge inversion at free salt ($\beta = 0$), and when the salt concentration is high, the charge inversion is noticed at $r = 24 \text{ \AA}$.

a)



b)

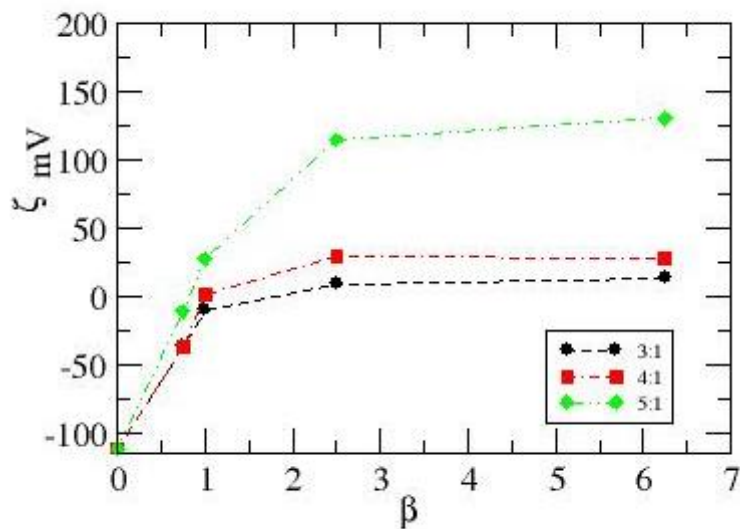


Figure 3.11: Electrostatic surface potential for the system at different values of β (0, 0.75, 1, 2.5 and 6.25) at 3:1, 4:1 and 5:1 salt ratios. At a) potential of the surface b) zeta potential equal.

In figure 3.11, the electrostatic potential increases when the concentration of electrolytes increases at different amounts of β , and then it becomes fixed at high values of β .

3.3 Critical surface charge density of the macroion:

When a surface is immersed in a solution containing electrolytes, it develops a net surface charge. This is often because of ionic adsorption. Aqueous solutions universally contain positive and negative ions (cations and anions, respectively), which interact with partial charges on the surface, adsorbing to and thus ionizing the surface and creating a net surface charge. This net charge results in a surface potential, which causes the surface to be surrounded by a cloud of counter-ions, which extends from the surface into the solution, and also generally results in repulsion between particles. The larger the partial charges in the material, the more ions are adsorbed to the surface, and the larger the cloud of counter-ions. A solution with a higher concentration of electrolytes also increases the size of the counter-ion cloud. This ion/counterion layer is known as the electric double layer.

For sufficiently large salt concentrations, the reversal of the colloidal charge will take place when the modulus of the colloidal surface charge density, $\sigma = Zq/4\pi r^2$, is larger than the critical value σ_c , which depends on the Bjerrum length, ionic radius, and the concentration of electrolyte through the scaling function $g(x, y)$.

$$\sigma_c = \frac{q}{a^2} g\left(\frac{a}{\lambda_B}, \lambda_B, \lambda_B C^{1/3}\right) \quad \text{Eq (3.5)}$$

This equation is particularly useful when one wants to obtain the critical surface charge density for suspensions with large concentrations of electrolyte. In these cases, the direct MC simulations become extremely slow due to large number of microions which must be used to simulate a *dilute* colloidal suspension.

It tells us that this critical surface charge density can also be obtained by simulating a much smaller system at a slightly lower temperature and with a somewhat larger microions. For example, suppose that we want to find the critical surface charge density of colloidal particles inside a dilute suspension at room temperature, $\lambda_B = 7.2 \text{ \AA}$, containing 3:1 electrolyte at concentration $C=1M$, with ions of radius of 2 \AA . Instead of doing the direct simulation of this system, we can simulate a “similar” system with say half the

number of microions, $C=0.5M$, at a slightly lower temperature, $\lambda_B = 7.2 \times 2^{1/3} = 9.07 \text{ \AA}$ and with ions of radius of $2 \times 2^{1/3} = 2.5 \text{ \AA}$. From Eq. 3.5, the critical charge of the original

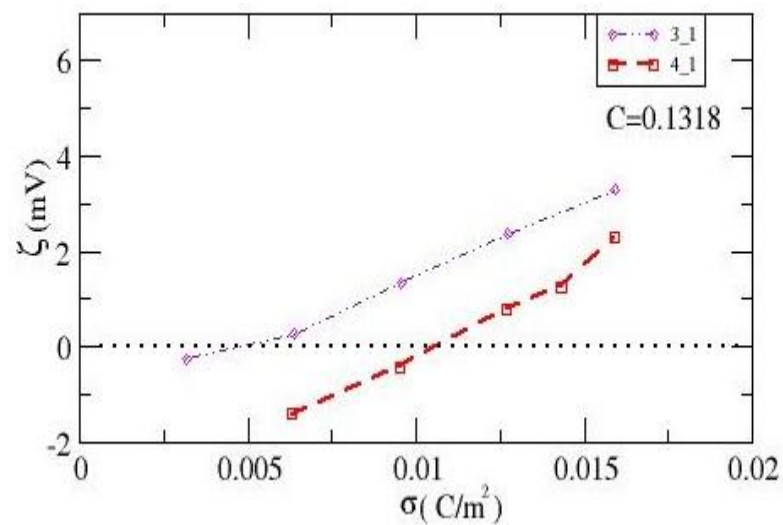
system (at concentration $C=1M$) will be $2^{2/3}$ times the critical charge of the similar system. The latter simulations, however, are much easier to perform since the number of microions involved is much smaller.

For weakly charged colloidal particles the increase in the surface charge density was accompanied by a uniform decline of the ζ potential accompanied the colloidal charge and became more negative. However, when the colloidal charge became sufficiently large, counterions condensation became important and ζ *increased* as a function of the bare colloidal charge, becoming positive for sufficiently strongly charged colloids.

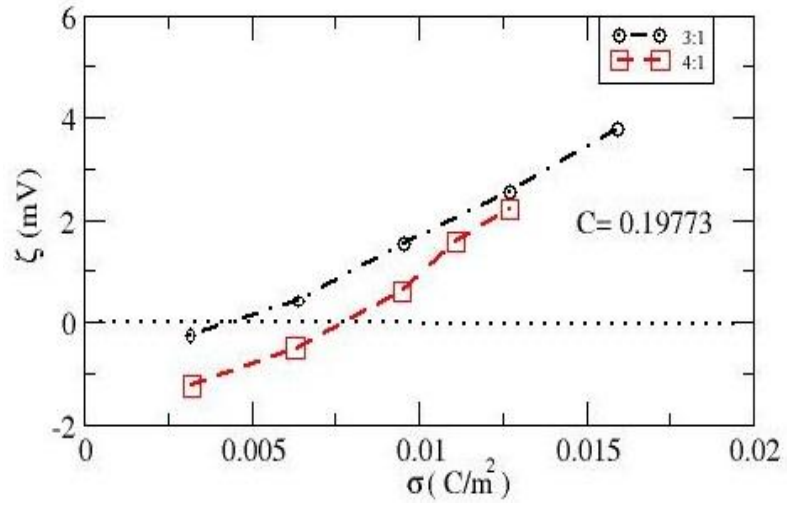
Figure3.12 accurately determines the critical colloidal charge density σ_c at which

$\zeta = 0$.

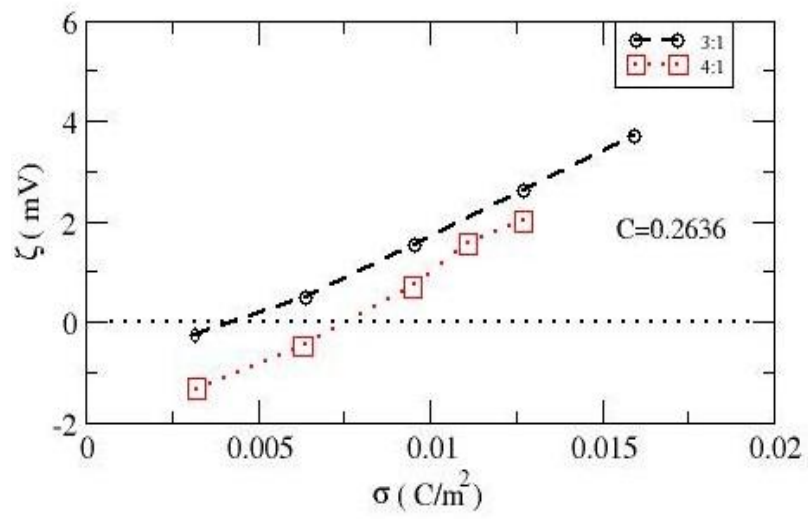
(a)



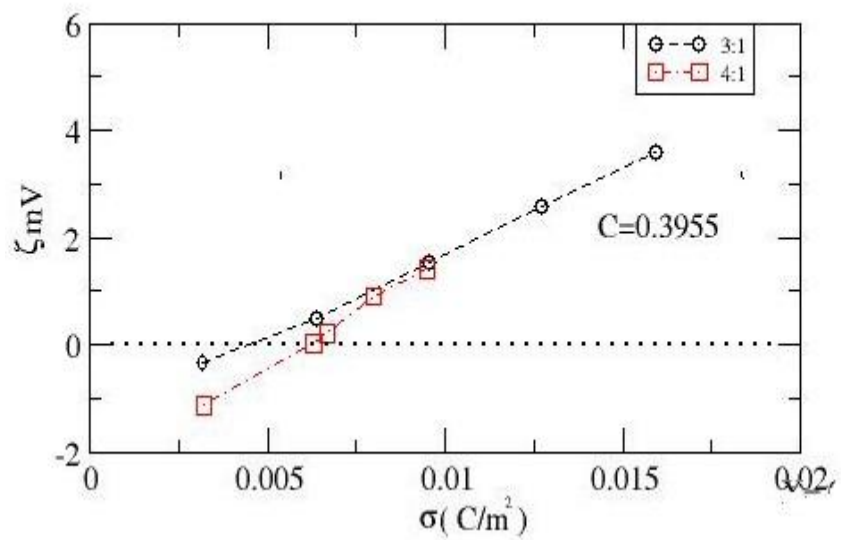
(b)



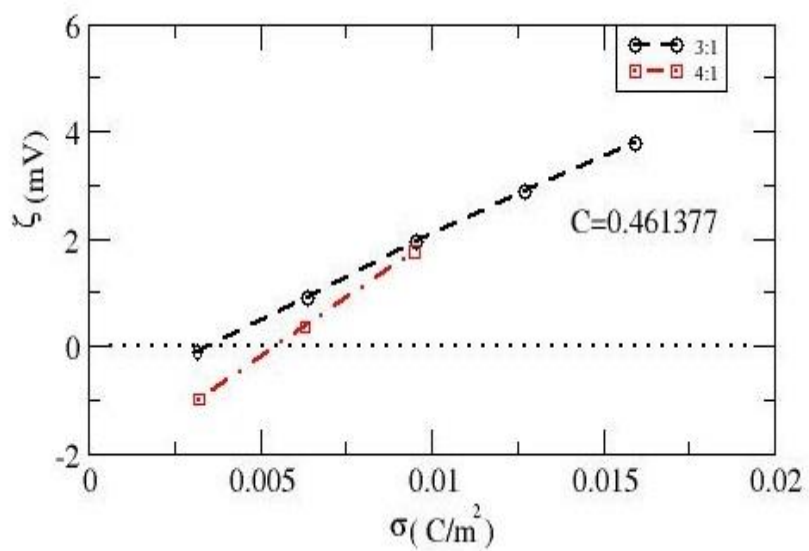
(c)



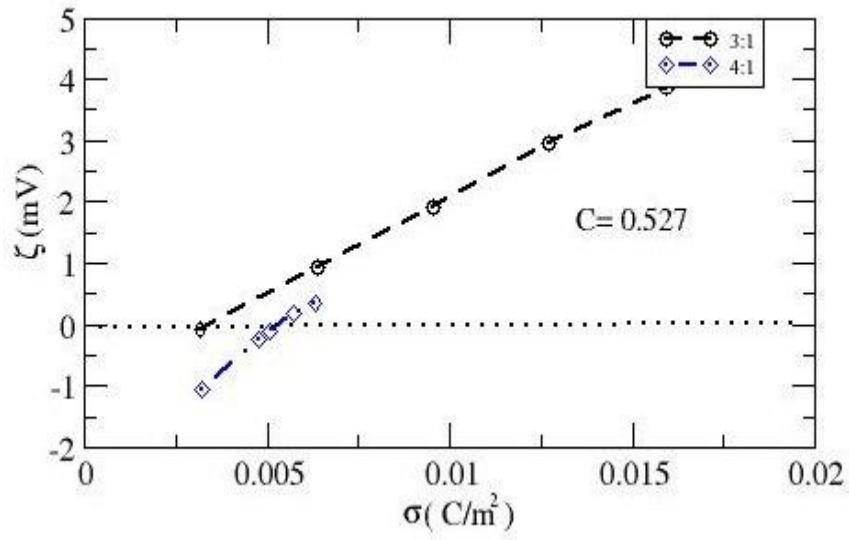
(d)



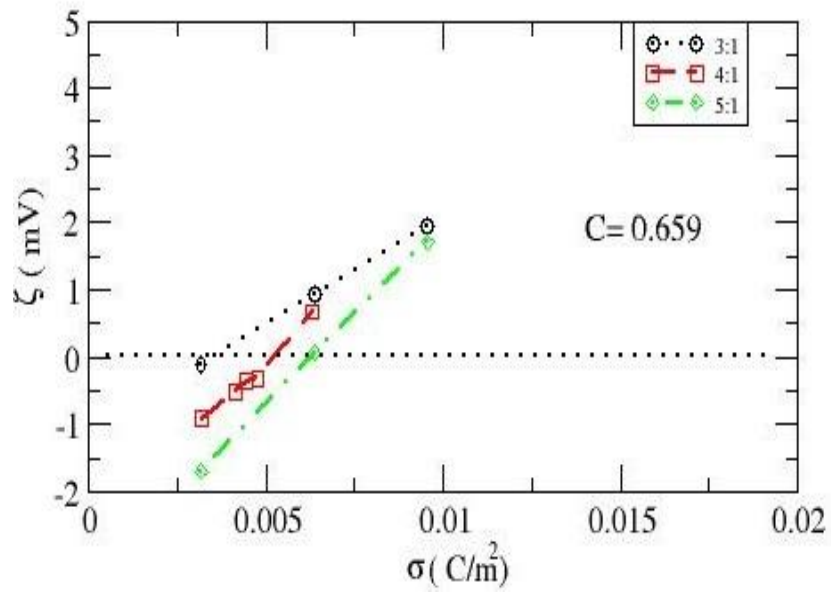
(e)



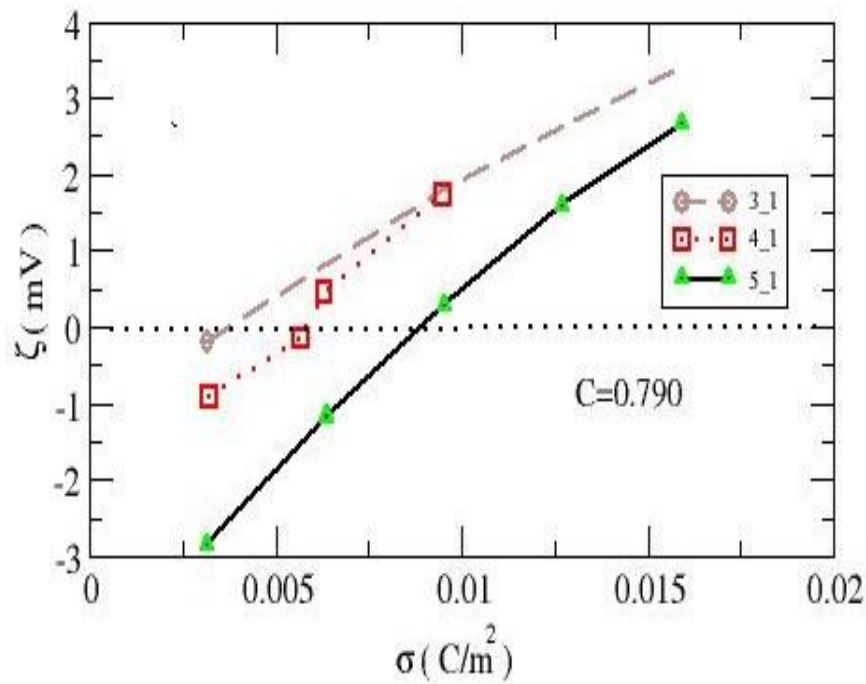
(f)



(g)



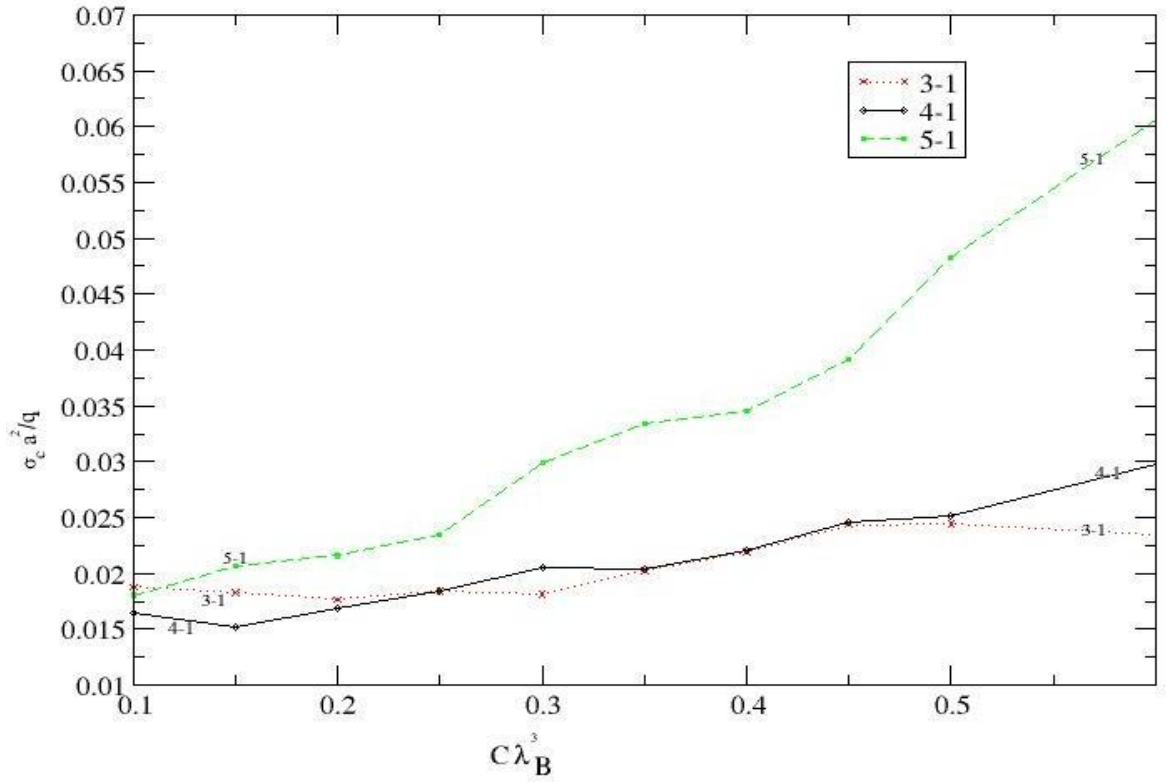
(h)



Figure(3.12): zeta potential as a function of the colloidal surface charge density at different molar concentrations indicated in figures a - h, and Bjerrum length is 10.8 \AA

In figure 3.12 we used a linear interpolation of the simulation data, and the results show that the value of colloidal surface charge density is 0.004 with 3:1 salt, whereas 0.006 with 4:1 salt, and it is 0.009 with 5:1 salt, at $C=0.790 \text{ M}$, these results made clear that the zeta potential increases when the surface charge density is increased in all systems, and its value is the highest with 5:1 salt, then with 4:1 salt, and finally with 3:1 salt.

In Fig.3.13 $(\sigma_c a^2 / q)$ is plotted as a function of $(C \lambda_B^3)$ for different electrolytes: $a = 2 \text{ \AA}$ and $\lambda_B = 10.8 \text{ \AA}$.



Figure(3.13): scaled colloidal surface charge density as a function of the scaled concentration of 3:1, 4:1, and 5:1 electrolyte.

Figure 3.13 shows that the value of σ_c is affected by the valence of the salt cations, with 5:1 salt σ_c is the highest, and with 3:1 salt it is the lowest. Also when the electrolyte concentration increases σ_c increases with all valences.

Chapter Four

Conclusion

Conclusions

Extensive Monte Carlo simulations and scaling arguments are used to study the colloidal charge reversal. The critical colloidal surface charge density σ_c at which the reversal first appears is found to depend strongly on the ionic size.

The electrostatic potential has been calculated between the macroion surface and the coincides ions in the solution. This value will be decayed when the counterions valances increase, and the salt concentration increase. It is observed that as the charge of counterions increases, the absolute value of electrostatic potential ψ_0 on the macroion surface decreases, analogues regularity is also traced for zeta potential ψ_d of the diffuse part.

The accumulated charge and the potential are affected with the high salt concentration due to the ions charges that increase in the solution. As the salt increases the potential and accumulated charge also increase. For multivalent counterions with high salt concentration, overcharging can be occurred.

For weakly charged colloidal particles increasing of the surface charge density was accompanied by a uniform decline of the ζ potential (ζ accompanied the colloidal charge and became more negative). However, when the colloidal charge became sufficiently large, counterion condensation became important and ζ *increased* as a function of the bare colloidal charge, becoming positive for sufficiently strongly charged colloids.

The critical surface charge density σ_c was found when ζ potential is zero.

In this work, the dependence of the critical surface charge density on the concentration of electrolyte was studied and the inversion of charge was noticed.

Future works will address the presence of added different types of salt, or using other boundary condition to study different properties of EDL structure. We can also change the distribution models with a new one with different radii and charges.

References

- 1- Kim YW, Yi J, Pincus PA (2008) Attractions between like-charged surfaces with dumbbell-shaped counterions. *Phys Rev Lett* 101:208–305.
- 2- May S, Iglic A, Rescic J, Maset S, Bohinc K (2008) Bridging equally charged macro-ions through long divalent rod-like ions. *J Chem Phys B* 112:1685–1692.
- 3- Grosberg.A.Y(2002), (2002). Nguyen.T.T, and Shklovskii.B.I, *Rev. Mod. Phys.* 74, 329 .
- 4- Urbanija J, Bohinc K, Bellen A, Maset S, Iglic A, Kralj-Iglic V, Sunil Kumar PBS (2008b) Attraction between negatively charged surfaces mediated by spherical counterions with quadrupolar charge distribution. *J Chem Phys* 129:105101.
- 5- Hatlo MM, Lue L (2009) A field theory for ions near charged surfaces valid from weak to strong couplings. *Soft Matter* 5:125–133.
- 6-Moreira AG, Netz RR (2002) Simulations of counterions at charged plates. *Eur Phys J E* 8:33–58
- 7- Bhuiyan LB, Outhwaite CW (2009) Comparison of exclusion volume corrections to the Poisson-Boltzmann equation for inhomogeneous electrolytes. *J Coll Int Sci* 331:543–547
- 8- Ibarra-Armenta JG, Martin-Molina A, Quesada-Perez M (2009) Testing a modified model of the Poisson-Boltzmann theory that includes ion size effects through Monte Carlo simulations. *Phys Chem Phys* 11:309–316.
- 9- Tresset G (2008) Generalized Poisson-Fermi formalism for investigating size correlation effects with multiple ions. *Phys Rev E* 78:061506.
- 10- (Deryaguin and Landau 1941) Deryaguin B. and Landau . D, (1941) : (A theory of the stability of strongly charged lyophobic sols and of the adhesion of strongly charged particles in solutions of electrolytes). "Acta Physicochim. USSR", Vol. 14, PP. 633-652.
- 11- (Verwey and Overbeek 1948) Verwey E. W. and Overbeek J. T. G., (1948): (theory of Stability of Lyophobic Colloids) Elsevier, Amsterdam.The Netherlands.
- 12- (Sogami and Ise 1984) Sogami I.,and Ise N., (1984): (On the electrostatic interaction in macroionic solutions)" *J. Chem. Phys*", Vol. 81:6, PP. 6320-6332.
- 13- (Lobaskin and Qamhieh2003) Qamhieh K. and Lobaskin V., (2003): (Effective Macroion Charge and Stability of Highly Asymmetric Electrolytes at Various Salt Conditions)" *J. Phys. Chem. B* ", Vol.107, PP.8022 -8028.

- 14- (Qamhieh and Linse 2005) Qamhieh K. and Linse P. , (2005) : (Effect of discrete macroion charge distributions in solutions of like-charged macroions) " J. CHEM. PHYS." Vol. 123, PP.104901.
- 15- . Perutkova´ et al(2010): Interaction of Membrane Surfaces, J Membrane Biol 236:43–53.
- 16- (Messina et.al. 2002) Messina R., Holm C., and Kremer K., (2002) : (Charge inversion in colloidal systems) "Computer Physics Communications" ,Vol. 147, PP. 282-285 .
- 17- (Messina et.al.(july)-2001) Messina R., Holm C., and Kremer K., (2001)(Strong electrostatic interactions in spherical colloidal systems) "Phys. Rev.E" ,Vol.64:2, PP.021405.
- 18 - (Molina et.al.2006) Molina A. M., Perez M. Q., and Alvarez R. H., (2006):(Electric Double Layers with Electrolyte Mixtures: Integral Equations Theories and Simulations)" J. Phys. Chem. B", Vol.110:3,PP. 1326-1331.
- 19- (Messina et.al. (March)-2001) Messina) R., Holm C., Kremer K., (2001): (Effect of colloidal charge discretization in the primitive model) "Eur. Phys. J. ", Vol. 4, PP 363-370 .
- 20 -Gelbart.M(2000), Bruinsma.R.F, Pincus.P.A, and Parsegian.V.A, Phys. Today 53, 38.
- 21- French R. H, Parsegian V.A, Podgornik.R, . Rajter.F, . Jagota.A, Luo.J, Asthagiri.D, M. K. Chaudhury, Y.-M. Chiang, S. Granick, et al. (2010). Rev. Mod. Phys. 82, 1887 .
- 22- (Diehl and Levin 2008) Diehl,A, Levin,Y,(2008):(Colloidal Charge Reversal Dependences on the Ionic Size and the Electrolyte Concentration), " J.Phys.Chem" Vol 129, PP 124566.
- 23- Angelini.T.E(2003), Liang.H, Wriggers.W, and .Wong.G.C.L, Proc. Nat. Acad. Sci. USA 100, 8634. A. E. Larsen (1997)and D. G. Grier, Nature 385, 230.
- 24- Terao.T (2001) and Nakayama.T, Phys. Rev. E 63, 041401.
- 25- Terao.T(2002) and Nakayama.T, Phys. Rev. E 65, 021405.
- 26- Zecheng Gan^{1,3}, Xiangjun Xing^{2,3}, and Zhenli Xu(2012), Effects of image charges, interfacial charge discreteness, and surface roughness on the zeta potential of spherical electric double layers, Shanghai 20024.
- 27- Tata.B.V.R(2008), Mohanty.P.S, and Valsakumar.M.C, Solid State Commun. 147, 360.
- 28- Gulbrand.L(1984), Jonsson.B, Wennerstro¨m.H, and Linse.P, J. Chem. Phys.**80**, 2221.

- 29- Wu.J.Z, D. Bratko(1989), and J. M. Prausnitz, Proc. Natl. Acad. Sci. USA **95**,15169.
- 30- Fenell-Evans .F and Wennerström.H(1994), The Colloidal Domain: Where Physics, Chemistry, Biology and Technology Meet.
- 31- Hiemenz.P.C and Rajagopalan.R, Principles of Colloid and Surface Chemistry (Marcel Dekker, New York,(1997).
- 32- Hunter.R.J(1981), Zeta Potential in Colloidal Science. Principles and Applications (Academic Press, London).
- 33- Lyklema.J(2009), Adv. Colloid Interface Sci. **147-148**, 205.
- 34- Lau.A.W.C(2002), Lukatsky.D.B, Pincus.P, and Safran.S.A, Phys. Rev. E **65**, 051502.
- 35- Labbez.C (2009), B. Jönsson.B, Skarba.M, and Borkovec.M, Langmuir **25**, 7209.
- 36- Van der Heyden.F.H.J (2006),. Stein.D, Besteman.K, Lemay.S.G, and Dekker.C, Phys. Rev. Lett. **96**, 224502.
- 37- Lopez-Garcia.J.J(2010), Aranda-Rascón.M.J, Grosse.C, and Horno.J, J. Phys. Chem. B **114**, 7548 .
- 38- (Lobaskin and Qamhieh 2002) Lobaskin,V, Qamhieh,K ,(2002): (Effective Macorion Charge and Stability of Highly Asymmetric Electrolytes at Various Salt Conditions)" J. Phys. Chem. B " , Vol 107, PP 8022 -8028.
- 39- Gouy.G(1910), J. Phys. **9**, 457 .
- 40-Chapman D.L(1913), Phil. Mag. **25**, 475.
- 41- Henderson.D(2005), Gillespie.D, Nagy.T, and Boda.D, [Mol. Phys.](#) **103**, 2851.
- 42- Moreira.A.G (2002)and Netz.R.R, [Europhys. Lett.](#) **52**, 705 _2000_; **57**, 911.
- 43- Fleck.C.C(2007) and Netz.R.R, [Europhys. Lett.](#) **70**, 341 _2005_; [Eur. Phys. J. E](#) **22**, 261.
- 44- S. Taheri-Araghi (2005) and B.-Y. Ha, [Phys. Rev. E](#) **72**, 021508.
- 45- NguyenT.T (2000), Grosberga A.Yu, and . Shklovskii.B.I, [Phys. Rev. Lett.](#) **85**, 1568 _2000_; [J. Chem. Phys.](#) **113**, 1110 .

أثر زيادة تركيز الملح على تغير شحنة الغرويات

إعداد: ريم عفانة.

إشراف: د. خولة قمحية

الملخص:

تهدف هذه الدراسة الى فحص تركيب الطبقة الكهربائية المزدوجة بالاتصال مع وسط جسم كروي مشحون من خلال إطار محدد من خلال محاكاة مونتج كارلو. لقد قمنا بدراسة تأثير تركيز الأملاح على تركيبة الطبقة الكهربائية المزدوجة وهذه التأثيرات تم تحليلها من خلال الأجسام الموجبة المتجمعة وكثافة الاشارات المشحونة والطاقة الكهربائية الكامنة.

* عندما تزداد قيمة الشحنات وايضا يزداد تركيز الملح تزداد الشحنات الكهربائية الفعالة.

* ونتيجة لذلك وعند زيادة حجم الشحنات وقيم بيتا لايونات الصغيرة تزداد القيمة المطلقة للطاقة الكهربائية الكامنة حتى تصل الى صفر عند الفصل الكبير للشحنات الموجودة على السطح والتي تؤثر على الطبقة الكهربائية المزدوجة وعلى كثافتها والتي تتناقص عندما تزداد قيمة الشحنة.

* عندما يزداد تركيز الملح يحدث انقلاب في شحنة الأيون الكبير حتى تتغير الشحنة الظاهرة الى الاتجاه المعاكس من الشحنة الأصلية من الأيون الكبير، والطاقة الكهربائية المحسوبة على السطح المحدد (٢٤ انجستروم) تتغير أيضا.